UNIVERSITY OF CRETE
FACULTY OF SCIENCES AND ENGINEERING
COMPUTER SCIENCE DEPARTMENT

Cooperation Incentives for Wireless Network Operators

Xenofon Fafoutis

Master of Science Thesis

Heraklion, February 2010

UNIVERSITY OF CRETE
FACULTY OF SCIENCES AND ENGINEERING
COMPUTER SCIENCE DEPARTMENT

Cooperation Incentives for Wireless Network Operators

A thesis submitted by

Xenofon Fafoutis

in partial fulfillment for the

Master of Science Degree

Author:

Xenofon Fafoutis

Commitee:

Apostolos Traganitis, Professor
Supervisor

Vasilios Siris, Assistant Professor
Athens University of Economics and Business
Advisor

Evangelos Markatos, Professor
Member

Accepted:

Panos Trahanias, Professor
Director of Graduate Studies

February 2010

Cooperation Incentives for Wireless Network Operators

Xenofon Fafoutis

Master of Science Thesis

Computer Science Department
University of Crete

Abstract

Wireless links, that operate at low transmission rates, become bottlenecks that degrade the end-to-end throughput, especially when they co-exist with high-rate links. Focusing in competitive environments where each party acts in its own self-interest and not towards a common goal, the objective of this thesis is to investigate the incentives for resourse sharing between operators of IEEE 802.11 networks with overlapping coverage. The analysis includes two types of wireless networks, namely wireless local area networks (WLANs) and wireless mesh networks (WMNs).

In the case of WLANs the investigation focuses on the incentives that can trigger handovers of wireless nodes that operate at low rates to neighboring access points that operate in the same channel but belong to other networks. The handovers address the well known problem in IEEE 802.11 networks, that the assignment of low-rate and high-rate users to the same access point significantly degrades the performance of the high-rate users. This fact gives rise to incentives for performing handovers, due solely to the improved performance handovers yield for both wireless networks.

In the case of backbone WMNs the investigation focuses on the incentives for mesh node sharing between different operators. Such cooperation aims to replace low-rate links with multiple higher rate links and can significantly improve the end-to-end throughput of both networks. The analysis includes both the case where only a limited number of channels are available, forcing mesh nodes to operate in the same channel, and the case where many orthogonal channels are available and their usage is constrained solely by the number of radios in each mesh node.

In order to investigate when such incentives arise for wireless networks operating in the same contention area, and to quantify the corresponding gains, a modeling framework is proposed. The modeling framework estimates the throughput of wireless nodes in IEEE 802.11 WLANs and the end-to-end throughput of a multi-hop WMN. It aims to identify the specific cases that either handovers or mesh node sharing yields performance improvements and advise the wireless network operators whether or not to share their resources. The analysis indicates that there can be significant performance improvements for both parties. The accuracy of the modeling framework is verified through simulations and experiments on a real test-bed.

Supervisor
Apostolos Traganitis
Professor

Computer Science Department
University of Crete

Κίνητρα Συνεργασίας Ανάμεσα σε Παρόχους Ασύρματων Δικτύων

Ξενοφών Φαφούτης

Μεταπτυχιακή Εργασία

Τμήμα Επιστήμης Υπολογιστών
Πανεπιστήμιο Κρήτης

Περίληψη

Οι ασύρματες ζεύξεις που λειτουργούν σε χαμηλούς ρυθμούς μετάδοσης δρουν περιοριστικά στην από άκρο σε άκρο απόδοση, ειδικά όταν συνυπάρχουν με ζεύξεις υψηλού ρυθμού. Εστιάζοντας σε ανταγωνιστικό περιβάλλον όπου κάθε πάροχος δρα σύμφωνα με το δικό του προσωπικό συμφέρον, στόχος αυτής της μεταπτυχιακής εργασίας είναι να ερευνηθούν τα κίνητρα συνεργασίας ανάμεσα σε παρόχους ασυρμάτων δικτύων τύπου IEEE 802.11 που το ένα επικαλύπτει το άλλο. Συμπεριλαμβάνονται δύο τύποι ασύρματων δικτύων, τα ασύρματα τοπικά δίκτυα και τα ασύρματα δίκτυα πλέγματος.

Στα ασύρματα τοπικά δίκτυα η έρευνα επικεντρώνεται στα κίνητρα που μπορούν να δώσουν το έναυσμα για την μεταβίβαση (handover) ασύρματων κόμβων που λειτουργούν σε χαμηλούς ρυθμούς σε γειτονικά Access Points που λειτουργούν στο ίδιο κανάλι αλλά ανήκουν σε διαφορετικό δίκτυο. Οι μεταβιβάσεις αντιμετωπίζουν το γνωστό πρόβλημα των δικτύων τύπου IEEE 802.11 , ότι η συνύπαρξη κόμβων που λειτουργούν σε χαμηλούς ρυθμούς με κόμβους που λειτουργούν σε υψηλούς ρυθμούς, υποβαθμίζει την απόδοση των τελευταίων. Το γεγονός αυτό δημιουργεί κίνητρα για μεταβιβάσεις, τα οποία βασίζονται μόνο στην βελτίωση της απόδοσης που επιφέρουν αυτές και στα δύο ασύρματα δίκτυα.

Στα ασύρματα δίκτυα πλέγματος η έρευνα επικεντρώνεται στα κίνητρα ώστε πάροχοι να εξυπηρετούν κίνηση γειτονικών παρόχων. Η συνεργασία αυτή έχει σαν στόχο να αντικαταστήσει ζεύξεις που λειτουργούν σε χαμηλούς ρυθμούς με πολλαπλές ζεύξεις που λειτουργούν σε υψηλούς ρυθμούς και μπορούν να βελτιώσουν σημαντικά την από άκρο σε άκρο απόδοση των δικτύων. Η μελέτη περιλαμβάνει την περίπτωση που υπάρχουν λίγα διαθέσιμα κανάλια που αναγκάζουν τις ζεύξεις να λειτουργούν στο ίδιο κανάλι, αλλά και την περίπτωση που υπάρχουν αρκετά διαθέσιμα ορθογώνια κανάλια όπου η χρήση τους περιορίζεται μόνο από τον αριθμό των κεραιών σε κάθε κόμβο.

Στοχεύοντας στον εντοπισμό των κινήτρων για παρόχους γειτονικών δικτύων, καθώς και στην ποσοτικοποίηση του κέρδους, προτείνεται ένα πλαίσιο μοντέλων. Τα μοντέλα εκτιμούν την από άκρο σε άκρο ρυθμαπόδοση των ασύρματων ζεύξεων και στοχεύουν στο να αναγνωρίσουν τις περιπτώσεις όπου η συνεργασία θα είναι επικερδής, έτσι ώστε να συμβουλεύουν τους παρόχους εάν τους συμφέρει να προχωρήσουν σε αυτή. Αναλυτικά πειράματα δείχνουν ότι υπάρχουν περιπτώσεις όπου η συνεργασία μπορεί να επιφέρει σημαντικές βελτιώσεις στην απόδοση και των δύο πλευρών. Η ακρίβεια του πλαισίου μοντέλων έχει επιβεβαιωθεί μέσω προσομοιώσεων και πραγματικών πειραμάτων.

Επόπτης
Απόστολος Τραγανίτης
Καθηγητής

Τμήμα Επιστήμης Υπολογιστών
Πανεπιστήμιο Κρήτης

Acknowledgements

I would like to thank my advisor, Vasilios A. Siris, for his guidance, support and our cooperation throughout the past two years. I would also like to thank my supervisor, Apostolos Traganitis, for his valuable advice. Lastly, I would like to express my gratitude to all of those who supported me in any respect during the completion of this thesis.

Contents

Acknowledgements **ix**

List of Figures **xiii**

List of Tables **xv**

Abbreviations **xvi**

1 Introduction **1**
1.1 Introduction . . . 1
1.2 Contribution . . . 2
1.3 Thesis Organization . . . 3

2 Related Work **5**
2.1 Related Work . . . 5

3 Handover Incentives in Wireless Local Networks **7**
3.1 Handover Incentives . . . 7
3.2 Throughput Model . . . 8
3.2.1 Objectives . . . 10
3.2.2 Simple Model for Downlink Direction . . . 10
3.2.3 Simple Model for Uplink Direction . . . 12
3.3 Other Topologies . . . 12
3.3.1 Three Access Points . . . 12
3.3.2 Mix of different low rate nodes . . . 14
3.3.3 No N_0 nodes . . . 16
3.3.4 Swapping low rate nodes . . . 17
3.4 Model Extensions . . . 18
3.4.1 Capacity Constraints . . . 18
3.4.2 Unsaturated Conditions . . . 20
3.4.3 Client Differentiation . . . 21
3.5 Analytical Investigations . . . 21
3.5.1 Node Density Model . . . 22
3.5.2 Evaluation Metric . . . 22
3.5.3 Analytical Investigations . . . 23
3.5.3.1 Base Scenario . . . 23
3.5.3.2 Effects of Density Model . . . 24

3.5.3.3 Different Topologies . . . 25
3.5.3.4 Capacity Constraints and Client Differentiation . . . 27
3.6 Simulation and Experimental Evaluation . . . 29
3.6.1 Simulations . . . 29
3.6.2 Experiments on Real Test-bed . . . 31
3.7 Implementation . . . 31
3.8 Conclusions . . . 33

4 Cooperation Incentives in Wireless Mesh Networks 35
4.1 Incentives in WMNs . . . 35
4.2 Throughput Model . . . 36
4.3 Single Channel . . . 37
4.3.1 Multiple Channels . . . 38
4.3.2 Capacity Constraints . . . 41
4.3.2.1 Single Channel . . . 42
4.3.2.2 Multiple Channels . . . 43
4.4 Analytical Investigations . . . 43
4.4.1 Single Channel . . . 44
4.4.2 Multiple Channels . . . 46
4.4.3 Capacity Constraints . . . 48
4.5 Simulation Evaluation . . . 49
4.6 Conclusions . . . 50

5 Conclusions and Further Work 53
5.1 Conclusions . . . 53
5.2 Further Work . . . 54

A Auxilliary Models 55
A.1 Protocol Overhead Model . . . 55
A.2 Physical Layer Model . . . 56

Bibliography 59

List of Figures

3.1 AP_0 serves both high-rate (N_0) and low-rate (N_0^x) users (*case a*). 8
3.2 AP_0's low-rate users (N_0^x) are handed-off to AP_1 (*case b*). 8
3.3 Three Access Points. No handovers performed (*case a*). 13
3.4 Three Access Points. Handovers performed (*case b*). 13
3.5 Mix of low-rate nodes. No handovers performed (*case a*). 14
3.6 Mix of low-rate nodes. Handovers of all low-rate nodes. 14
3.7 Mix of low-rate nodes. Handovers of the nodes that operate at r_1, $r_1 < r_2$. 15
3.8 No N_0 nodes. No handovers performed (*case a*). 16
3.9 No N_0 nodes. Handovers performed (*case b*). 16
3.10 Swapping low rate nodes. No handovers performed (*case a*). 17
3.11 Swapping low rate nodes. Handovers performed (*case b*). 17
3.12 Base scenario in 802.11b and 802.11a. 23
3.13 Threshold c in 802.11b. All areas below each line refer to beneficial scenarios. . . 24
3.14 Base scenario in 802.11b for different objectives. 24
3.15 Experimenting on the *mean* of the node density model. 25
3.16 Experimenting on the *variance* of the node density model. 25
3.17 Three access points in 802.11b. 26
3.18 Mix of low rate nodes where $r_1 = 1$ Mbps in 802.11b. 26
3.19 No N_0 nodes in 802.11b. 27
3.20 Swapping low rate nodes in 802.11b. 27
3.21 Capacity constraints in 802.11a where $r = 6$ Mbps and $C_0 = 54$ Mbps. 28
3.22 Capacity constraints in 802.11a where $r = 6$ Mbps and $C_1 = 54$ Mbps. 28
3.23 Client differentiation by AP_1 in 802.11b where $r = 1$ Mbps. 29
3.24 Comparison of model estimations and simulations. 30
3.25 Comparison of model estimations and experiments. 31
3.26 Handover process in AP_1. 32
3.27 Implementation of handover process. 33

4.1 No Mesh Node Sharing (*Case a*). 36
4.2 Mesh Node Sharing (*Case b*). 36
4.3 Multi-channel, 1-radio nodes, no mesh node sharing. 39
4.4 Multi-channel, 1-radio nodes, mesh node sharing. 39
4.5 Multi-channel, 2-radio nodes, no mesh node sharing. 40
4.6 Multi-channel, 2-radio nodes, mesh node sharing. 40
4.7 Multi-channel, 3-radio nodes, no mesh node sharing. 41
4.8 Multi-channel, 3-radio nodes, mesh node sharing. 41
4.9 Throughput gain as a function of $x = d_{A_1B_2}$; $d_{A_1A_2} = d_{B_1B_2} = 541$ m, single channel, 802.11b. 44

4.10 Throughput gain as a function of $x = d_{A_1B_2}$; $d_{A_1A_2} = d_{B_1B_2} = 368$ m, single channel, 802.11a. 45
4.11 Throughput gain as a function of $x = d_{A_1B_2}$, when nodes A_1, A_2 can communicate at rate 11 Mbps; single channel, 802.11b 45
4.12 Throughput gain as a function of $x = d_{A_1A_2} = d_{B_1B_2}$, while $d_{A_1B_2} = x/2$; single channel, 802.11b 46
4.13 Throughput gain as a function of the path loss exponent; $d_{A_1A_2} = d_{B_1B_2} = d_{max}$, $d_{A_1B_2} = d_{max}/2$, single channel. 46
4.14 Throughput gain as a function of $x = d_{A_1B_2}$; $d_{A_1A_2} = d_{B_1B_2} = 368$ m, single-radio, 802.11a. 47
4.15 Throughput gain as a function of $x = d_{A_1B_2}$; $d_{A_1A_2} = d_{B_1B_2} = 368$ m, 2-radio, 802.11a. 47
4.16 Throughput gain as a function of $x = d_{A_1B_2}$; $d_{A_1A_2} = d_{B_1B_2} = 368$ m, 3-radio, 802.11a. 48
4.17 Throughput gain as a function of $x = d_{A_1B_2}$; $d_{A_1A_2} = d_{B_1B_2} = 541$ m, single channel, 802.11b, $C_A = 5$ Mbps. 48
4.18 Throughput gain as a function of C_A; $d_{A_1B_2} = 270$ m, $d_{A_1A_2} = d_{B_1B_2} = 541$ m, single channel, 802.11b. 49
4.19 Gain based on analysis and simulation. 50

List of Tables

4.1 Transmission rates (in Mbps) for various links, in different experiments. 49

A.1 Delay components for transmitting one frame in 802.11a. 56
A.2 Delay components for transmitting one frame in 802.11b. 56
A.3 Sensitivity thresholds for 802.11a 57
A.4 Sensitivity thresholds for 802.11b 57

Abbreviations

ADSL	Asymmetric Digital Subscriber Line
AP	Access Point
CTS	Clear To Send
DCF	Distributed Coordination Function
DSL	Digital Subscriber Line
DSLAM	Digital Subscriber Line Access Multiplexer
EIRP	Equivalent Isotropically Radiated Power
ETSI	European Telecommunications Standards Institute
IFS	Inter-frame Space
LAN	Local Area Network
MAC	Media Access Control
MIMO	Multiple Input Multiple Output
NS	(The) Network Simulator
PLCP	Physical Layer Convergence Protocol
RSSI	Received Signal Strength Indication
RTS	Request To Send
UDP	User Datagram Protocol
WLAN	Wireless Local Area Network
WMN	Wireless Mesh Network

Chapter 1

Introduction

1.1 Introduction

In wireless networks, low transmission rate links create bottlenecks that degrade the end-to-end throughput. Additionally, the co-existence of low and high-rate links operating in the same channel can significantly degrade the throughput of the latter. It is well known that in IEEE 802.11 networks, the assignment of low and high transmission rate users to the same access point significantly degrades the performance of the high-rate users [FRBsD03]. This occurs because IEEE 802.11's medium access control protocol gives both high and low-rate nodes equal chances for accessing the shared wireless channel. However, low-rate nodes need more time to send the same amount of data. As a result, high-rate users suffer significant performance degradation, achieving throughput equal to that of low-rate users.

The objective is to investigate the incentives for resource sharing between operators of IEEE 802.11 networks with overlapping coverage. Through such cooperation, the low-rate links are replaced by higher rate links. Hence, not only the performance of the clients that operate at low rates is improved, but the throughput degradation due to the performance anomaly is avoided. Of course, such cooperation between operators can also result from agreements that involve monetary exchange or interconnection agreements similar to those that exist between telephony operators. However, the focus of our work is on the cooperation incentives due *solely* to the improved performance that cooperation yields for *both* wireless networks. The existence of such performance-oriented incentives have important implications, since they can trigger cooperation between wireless network operators that act in their own self-interest.

We investigated the performance-oriented incentives for cooperation in two types of wireless networks. In overlapping IEEE 802.11 wireless local area networks (WLANs), handovers of wireless nodes that operate at low rates to neighboring access points that belong to other

networks can improve the performance of both parties. Hence, this performance improvement can motivate a cooperation between different parties that act at their own self-interest. In wireless mesh networks (WMNs) we investigate the incentives for mesh node sharing between different operators. Such cooperation aims to replace low-rate links with multiple higher rate links, and is induced solely from the improved performance that can be achieved through sharing of resources.

In order to investigate when such incentives arise for wireless networks operating in the same contention area, and to quantify the corresponding gains, we propose a modeling framework which estimates the throughput of wireless nodes in IEEE 802.11 WLANs and the end-to-end throughput of a multi-hop wireless mesh network. A key feature of the model is that it captures the effects of rate diversity on the throughput. Our modeling framework aims to identify the specific cases that cooperation yields performance improvements and consult the wireless network operators whether or not to proceed to the cooperation.

1.2 Contribution

The main contribution of this thesis lies in the incentives that arise by the fact that resource sharing between competitive operators can yield significant performance improvements. The key difference to prior work is the focus on competitive parties that act at their own self-interest and there is no other cooperation between them, such as monetary exchange or other forms of enforcement. Prior work, on one hand, aims to improve the performance of single networks or cooperative networks that work towards a common goal. Prior work in competitive environments, namely ad-hoc wireless networks, focuses on ways to enforce cooperation. The focus of this thesis, on the other hand, is to identify when cooperation can be motivated solely by performance improvements; hence, without requiring any other form of cooperation. Related work is further discussed in the next chapter.

An additional contribution lies in the analytical framework used to identify and quantify the scenarios where resource sharing is beneficial for both parties. Although throughput approximation methods that capture rate diversity have been used in [KAMG07], [KK05], [KKN06], [KBC+07] and [KS08], these works focus solely on the case of simple scenarios that include a single wireless hop. On the other hand, the model proposed in this thesis includes various topologies and conditions such as capacity constraints, client differentiation and unsaturated conditions. Additionally, in the case of WMNs the throughput model proposed considers the end-to-end throughput across multiple wireless hops.

1.3 Thesis Organization

The remainder of this thesis is organized as follows. Chapter 2 summarizes the related work. Chapter 3 investigates the handover incentives in IEEE 802.11 wireless local area networks. Chapter 4 investigates the performance incentives in IEEE 802.11 based wireless mesh networks. Each chapter consists of a section which describes the modeling framework, a section which presents analytical investigation based on the model and a section which evaluates the model. Finally, Chapter 5 concludes the thesis.

Chapter 2

Related Work

2.1 Related Work

In this chapter the related work is briefly summarized. This work does not focus centrally on the performance-oriented incentives that can motivate resource sharing, which is the focus of this thesis. Rather, one line of work investigates approaches for improving the performance in wireless networks, whereas another line of work considers token or virtual currency based approaches for inducing cooperation.

The handover incentives and cooperation incentives in overlapping WMNs that operate at the same channel address the performance degradation problem of 802.11 networks [FRBsD03] from a new perspective. Related work has approached the same issue in different ways.

One approach mitigates the performance anomaly by making use of relay nodes for transmissions that cannot be performed at high rates [NLP05][LTN+07][LL05][FCH+07][BCL+08]. In [LL05] the authors propose a centralized protocol named Relay-based Adaptive Auto Rate (RAAR). Each node observes the RSSI of its neighbors and estimates the transmission rate for communicating with them; this information is forwarded to the access point which assigns relay nodes. In [FCH+07] the authors suggest an approach that allows nodes to increase their performance by replacing one low-rate transmission with a sequence of two high-rate transmissions. Each transmitter opportunistically makes frames available for relaying without any prior relay discovery. In [BCL+08] the authors present an approach where high-rate nodes opportunistically turn themselves into repeaters for low-rate nodes, hence requires the availability of such relay nodes. The focus is on enabling the repeater functionality only when it is beneficial for both the repeater and the low-rate clients. The nodes are assumed to cooperate to achieve a common goal, such as to maximize the aggregate throughput and max-min fairness.

The above works focus on a single WLAN and they can be effective when the relay nodes are

available. The handovers incentives are effective when different conditions arise. In any case, we focus on the co-existence of wireless networks that belong to different operators. These wireless networks operate in competitive environments where each party acts in its own self-interest, and not towards a common goal.

Another approach to mitigate the problem is to reduce the time low-rate transmissions utilize the shared medium, thus providing time fairness [SS06][TG04]. Although such an approach can increase the aggregate throughput of the network, it is unfair to low-rate nodes, as it decreases further their performance. This leads to unsatisfied clients, which should be avoided in an environment with multiple competing providers.

Another approach is to aggregate the capacity of all the access points and use load balancing mechanisms in order to maximize the network performance [DVR03][BPK$^+$07][KLBK08]. Moreover, in wireless mesh networks, routing metrics such as ETT [DPZ04], WCETT [DPZ04] and CATT [GS08], take the transmission rate into account. Routing protocols using these metrics would choose to route traffic through high-rate links, avoiding low-rate links. These approaches requires all access points / mesh nodes to cooperate, which can be assumed in the case where they belong to the same operator, but not when they belong to different operators. On the other hand, our focus is exactly on the cooperation between different operators, and shows that such cooperation can result from performance-oriented incentives even when operators act in their own self-interest.

Mobile ad hoc networks is a field where every node can act in its own interest and the cooperation incentives are important. One direction assures cooperation using a token-based incentive system [BH03][CGKO04]. The key concept of this approach is to earn credits when forwarding traffic for others and spend them in order to buy forwarding services from others. Some systems also propose using real money as credit [ZCY03]. Trust management systems [AE03][ByLB02] is another approach for inducing cooperation. These systems support reputation mechanisms in order to detect and punish nodes that misbehave. A key idea and motivation for our work is that such mechanisms are not required in overlapping wireless networks, when performance improvements alone can provide sufficient cooperation incentives.

Chapter 3

Handover Incentives in Wireless Local Networks

3.1 Handover Incentives

In the case of IEEE 802.11 WLANs with overlapping coverage and assuming that both networks operate at the same channel, low rate clients not only degrade the performance of the high rate clients of their network, but also degrade the performance of the high rate clients of the neighboring network. This fact arises incentives for supporting handovers, due solely to the improved performance handovers yield for both wireless networks.

The main assumption of these scenarios is that two or more access points operate in the same channel. Indeed, it is common that there are more than three access points within the range of each other [AJSS05]. Hence, the three orthogonal channels available in 802.11b and 802.11g are not sufficient to assign orthogonal channels to different access points. Moreover, as more wireless networks operating in unlicensed bands are deployed over time, the above scenario will be more dominant.

The chapter includes modeling and complete analysis of the downlink direction in a basic scenario that includes two access points and three sets of nodes. Based on the necessary conditions for a handover to be beneficial for both access points, we propose a policy that can be used by each access point in order to decide whether to accept the handover. A series of analytical investigation illustrate the important trends and tradeoffs. Moreover, the accuracy of the modelings framework is evaluated through simulations and real experiments.

Additionally to the basic scenario, the contributions of this chapter include:

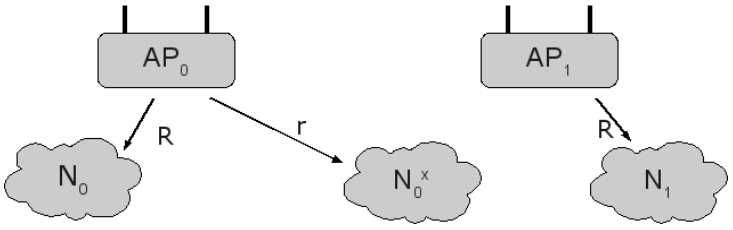

FIGURE 3.1: AP_0 serves both high-rate (N_0) and low-rate (N_0^x) users (*case a*).

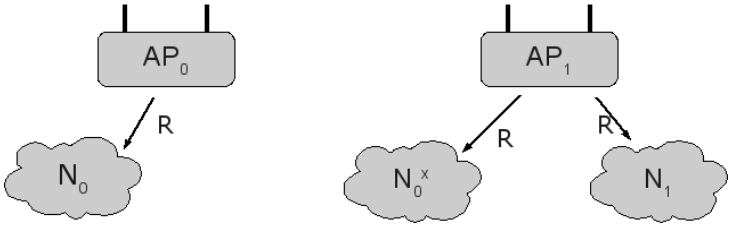

FIGURE 3.2: AP_0's low-rate users (N_0^x) are handed-off to AP_1 (*case b*).

- Investigation on multiple performance objectives, such throughput maximization and fairness.
- Analysis of the uplink direction.
- Further analysis of the trade-offs and the trends of the handovers by the investigation of alternative topologies such as three access points and low rate clients with different transmission rates.
- Modeling and analysis of the implications of capacity constraints external to the wireless domain.
- Investigation on scenarios where the access points transmit traffic in a constant bit rate instead of saturated conditions.
- Investigation on the use of priority mechanisms by the host of the guest clients.

3.2 Throughput Model

Consider the case of two access points, AP_0 and AP_1, Figure 3.1. AP_0 sends traffic to N_0 nodes at high rate R and to N_0^x nodes at low rate r. Nodes N_0 and N_0^x are the clients of AP_0 and its actions target to improve their throughput. AP_1 sends traffic to nodes N_1 at high rate R. Nodes N_0^x are closer to AP_1 and would transmit at a higher rate R, if they were associated to it. This is the base scenario, which we will refer to as *case a*. Other scenarios are investigated later in this chapter. Additionally, the following assumptions are made: (a) both access points operate at the same channel, (b) all access points and nodes are in the same contention area and

(c) there is at least one node in each of the three node sets. Due to the low-rate transmissions to the set of N_0^x nodes, the performance for all N_0 and N_1 nodes degrades.

This topology is the basic scenario we investigate. The objective is to identify when both parties have performance-oriented incentives that can trigger the handovers of the low rate clients (N_0^x) of AP_0, to the neighboring access point AP_1. This is the scenario shown in Figure 3.2, which we will refer to as *case b*. Now, AP_1 sends traffic only to the N_0 nodes at high rate R, while AP_1 sends traffic at high rate R to both its own clients (N_1) and the ex-low-rate clients of AP_0 (N_0^x).

The throughput gain of AP_i is defined as the ratio of the aggregate utilities of the throughput of the clients of AP_i in *case b* (Nx clients associated to AP_1), over the utilities in *case a* (N_0^x clients associated to AP_0). This metric is used in order to evaluate when the handover of low-rate users (*case b*) is beneficial. When the gain for both access points is greater than 1, handover improves the aggregate utilities of the clients of both access points. For AP_0 the gain is estimated by

$$Gain_{AP_0} = \frac{N_0 \cdot u(X^b_{N_0}) + N_0^x \cdot u(X^b_{N_0^x})}{N_0 \cdot u(X^a_{N_0}) + N_0^x \cdot u(X^a_{N_0^x})} \,, \tag{3.1}$$

where $u(\cdot)$ is the utility function and X is the respective estimated throughput. It is important to note that the N_0^x nodes are clients of AP_0 in both cases, even though in the second case they are associated to AP_1. For AP_1 the gain is estimated by

$$Gain_{AP_1} = \frac{u(X^b_{N_1})}{u(X^a_{N_1})} \,. \tag{3.2}$$

The throughput model considers the function $T(p, R)$, which denotes the expected duration for the transmission of a frame with payload size p, when the 802.11 transmission rate is R. If we disregard all overheads, this function is given by

$$T(p, R) = \frac{p}{R} \,. \tag{3.3}$$

The last expression captures a key property of wireless networks, namely that the duration of a packet transmission is higher for nodes with a smaller transmission rate. Appendix A.1 presents an expression for $T(p, R)$ that includes all protocol overheads.

The analysis in the following sections focuses on the above simple model, which encompasses the key tradeoffs we want to highlight.

3.2.1 Objectives

The expression of the utility function, $u(\cdot)$, depends of the objectives of the operators of the wireless networks.

When the objective of each operator is the maximization of the aggregate throughput of its respective clients, the utility function of each client is expressed by

$$u(x) = x \ ,$$

where x is its throughput.

When the operators want to provide fairness among their clients, the utility function is concave. A concave utility function indicates that extra throughput is less valuable as more throughput is achieved. In this case, the utility function of each client is expressed by

$$u(x) = \ln x \ ,$$

where x is its throughput.

3.2.2 Simple Model for Downlink Direction

Next we present a model for the throughput in saturated conditions for the downlink direction, i.e., from the access points to the clients. We assume that each access point sends one packet in each round. This is not absolutely true for IEEE 802.11 since the backoff waiting time of each transmission, as defined by the collision avoidance mechanism, is decided probabilistically. However, since the DCF protocol of IEEE 802.11 provides long term fair channel access, the access points will send an equal amount of packets over a long time interval.

***case a* (no handover):** When N_0^x nodes are assigned to AP_0, the expected time interval that AP_0 needs to transmit a packet depends on the percentage of traffic sent to N_0 and N_0^x nodes, since the duration of the transmission is different due to the different rates. On the other hand, the expected time interval that AP_1 needs to transmit a packet is independent of the number of its nodes since all operate at the same rate. The long term throughput in bits per second that each access point will achieve, namely X^a, assuming both access points transmit packets of the same size, is given by

$$X^a = \frac{p}{\frac{N_0}{N_0+N_0^x} \cdot T(p,R) + \frac{N_0^x}{N_0+N_0^x} \cdot T(p,r) + T(p,R)} \ , \tag{3.4}$$

where N_0 and N_0^x are the number of nodes in the N_0 and N_0^x node-set respectively. The expected throughput of each node in N_0, N_0^x and N_1 is

$$X^a_{N_0} = X^a_{N_0^x} = \frac{1}{N_0 + N_0^x} X^a \,, \qquad X^a_{N_1} = \frac{1}{N_1} X^a \,, \tag{3.5}$$

where X^a is estimated from (3.4).

***case b* (handover of low rate users):** In the case that the low rate nodes are handed over, the long term throughput that each access point will achieve, namely X^b, is equal to

$$X^b = \frac{p}{2 \cdot T(p, R)} \,. \tag{3.6}$$

The expected throughput of each node in N_0, N_0^x and N_1 is

$$X^b_{N_0} = \frac{1}{N_0} X^b \,, \qquad X^b_{N_0^x} = X^b_{N_1} = \frac{1}{N_0^x + N_1} X^b \,. \tag{3.7}$$

The gain of each access point is calculated by assigning the respective estimated throughput (3.5) and (3.7) to (3.2) with respect to the objective as discussed in Section 3.2.1.

The key tradeoff is the following. When low-rate nodes are associated to AP_0 (*case a*), throughput is reduced. On the other hand, when the low-rate nodes are associated with AP_1 (*case b*), AP_1 shares its share of the wireless channel with the N_0^x nodes, which are AP_0's clients. It is obvious that *case b* is always beneficial for AP_0 when the objective is throughput maximization, since AP_0's clients not only utilize the wireless channel for more than half of the time, but the throughput also improves due to removing low-rate transmissions. The following inequalities

$$Gain_{AP_0} = \frac{X^b + \frac{N_0^x}{N_0^x + N_1} X^b}{X^a} > 1 \;\text{ and }\; Gain_{AP_1} = \frac{\frac{N_1}{N_0^x + N_1} X^b}{X^a} > 1 \tag{3.8}$$

are necessary conditions for handover to be beneficial for both access points, assuming that the objective is throughput maximization ($u(x) = x$). Since $X^b > X^a$, the $Gain_{AP_0} > 1$ is always satisfied. However, if the assumption $N_0 > 0$ does not hold, then *case b* is not always beneficial for AP_0. The second inequality $Gain_{AP_1} > 1$ is equivalent to

$$\frac{N_1}{N_0^x + N_0} > c \,, \;\text{ where }\; c = \frac{2}{\frac{R}{r} - 1} \,. \tag{3.9}$$

where c is a factor that depends on the rate of the low-rate transmissions, the maximum rate and the packet size.This inequality can be used by AP_1 to decide if it is beneficial to serve the low-rate nodes of his neighboring access point AP_0. We make an interesting remark regarding the above constraint. The acceptance constraint does not depend on the ratio of high-rate to low-rate nodes of AP_0, but depends only on their sum.

3.2.3 Simple Model for Uplink Direction

In the uplink direction, each node contends for the wireless medium. Assuming each client transmits one frame in each round, for *case a* the throughput of each node is:

$$X^a_{N_0} = X^a_{N_0^x} = X^a_{N_1} = \frac{p}{N_0 \cdot T(p,R) + N_0^x \cdot T(p,r) + N_1 \cdot T(p,R)}$$

For *case b* the throughput is:

$$X^b_{N_0} = X^b_{N_0^x} = X^b_{N_1} = \frac{p}{N_0 \cdot T(p,R) + N_0^x \cdot T(p,R) + N_1 \cdot T(p,R)}$$

Obviously, as long as $R > r$, the gain inequality $Gain > 1$ is always satisfied regardless the utility function, indicating that the handover is always beneficial for every node.

3.3 Other Topologies

In this section we study alternative topologies using variations of the above model in order to highlight the trends of the handovers in multiple situations. The alternative topologies include the scenarios of three access points in the same contention area, the case where a different low rate nodes co-exist in the same contention area, the case where the number of the nodes in N_0 set is zero and the case where AP_1 has also low rate nodes that are close to AP_0.

3.3.1 Three Access Points

Assume now that there is a third access point, AP_2 in the same contention area, operating at the same channel. This scenario, indeed, is less frequent than the base scenario since it assumes that there are three access points operating at the same channel. Assuming that there are three orthogonal channels, at least seven access points operating in the same area are required.

This access point serves N_2 nodes at rate R and acts towards their interests, Fig. 3.3. Additionally we assume that some of the N_0^x are close to AP_1 and the other close to AP_2. Consider that N_0^y nodes can operate at high rate R when handed over to AP_1. The rest $N_0^z = N_0^x - N_0^y$ nodes can be handed off to AP_2. We also assume that $N_0^y > 0$ and $N_0^z > 0$. There are now three contending transmitters in the downlink direction.

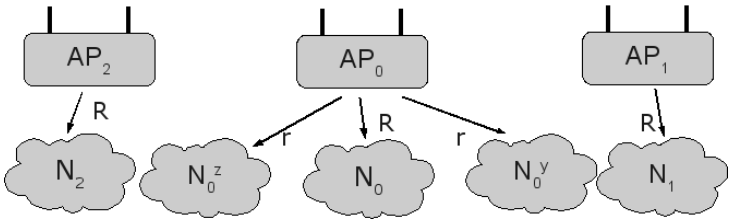

FIGURE 3.3: Three Access Points. No handovers performed (*case a*).

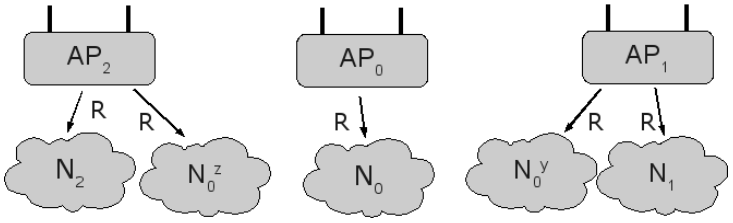

FIGURE 3.4: Three Access Points. Handovers performed (*case b*).

***case a* (no handover):** For the baseline scenario and since there is per-packet fairness, the long-term throughput of each access point is estimated by

$$X^a = \frac{p}{\frac{N_0}{N_0+N_0^x} \cdot T(p,R) + \frac{N_0^x}{N_0+N_0^x} \cdot T(p,r) + 2 \cdot T(p,R)} \,. \tag{3.10}$$

We note that since all clients associated with AP_2 are served at the same rate, R, the duration that AP_2 uses the medium is equal to $T(p,R)$; the same holds with AP_1.

The expected throughput of each node in N_0, N_0^x, N_1 and N_2 is estimated by

$$X^a_{N_0} = X^a_{N_0^x} = \frac{1}{N_0 + N_0^x} X^a \,, \quad X^a_{N_1} = \frac{1}{N_1} X^a \,, \quad X^a_{N_2} = \frac{1}{N_2} X^a \,,$$

where X^a is estimated by (3.10).

***case b* (handover of low rate nodes):**

Next we consider that the neighboring access points cooperate and accept to serve the low rate nodes that are close to them, Fig. 3.4. The N_0^y nodes are handed off to AP_1 and the remaining N_0^z nodes are handed off to AP_2. All nodes transmit at rate R and, as a result, the estimated throughput of each access point is estimated by

$$X^b = \frac{p}{3 \cdot T(p,R)} \,. \tag{3.11}$$

The estimated throughput for each node in N_0, N_0^y, N_1, N_0^z and N_2 is

$$X^b_{N_0} = \frac{1}{N_0} X^b \,, \quad X^b_{N_0^y} = X^b_{N_1} = \frac{1}{N_0^y + N_1} X^b \,, \quad X^b_{N_0^z} = X^b_{N_2} = \frac{1}{N_0^z + N_2} X^b \,,$$

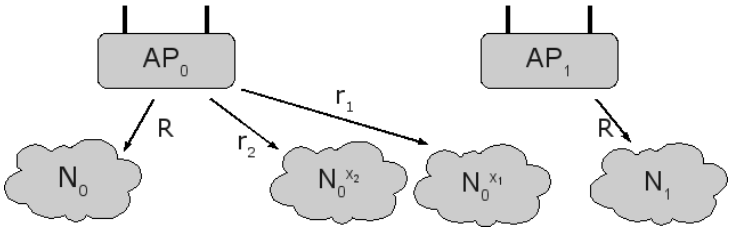

FIGURE 3.5: Mix of low-rate nodes. No handovers performed (*case a*).

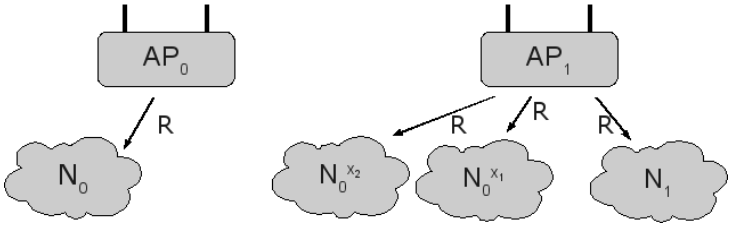

FIGURE 3.6: Mix of low-rate nodes. Handovers of all low-rate nodes.

where X^b is estimated by (3.11).

The following inequalities are necessary conditions for the handovers to be beneficial for the clients of all three access points, assuming that the objective is throughput maximization ($u(x) = x$).

$$Gain_{AP_0} = \frac{X^b + \frac{N_0^y}{N_0^y+N_1}X^b + \frac{N_0^z}{N_0^z+N_2}X^b}{X^a} > 1 \text{ and}$$

$$Gain_{AP_1} = \frac{\frac{N_1}{N_0^y+N_1}X^b}{X^a} > 1 \text{ and } Gain_{AP_2} = \frac{\frac{N_2}{N_0^z+N_2}X^b}{X^a} > 1$$

We observe that the handover is not always beneficial for the third access point, similarly to AP_1. There is a new tradeoff in this case. The existence of an additional access point decreases the time the low rate nodes use the medium, thus tends to make handovers less beneficial. On the other hand, the low-rate nodes are shared between the two access point in *case b*. The latter tends to make handovers more beneficial comparing to the base scenario.

3.3.2 Mix of different low rate nodes

This variation considers the case where a mix of different low rate nodes co-exist in the same contention area. For instance, a mix of nodes operating at 1 Mbps and 5.5 Mbps in 802.11b. We assume that AP_0 has three client sets assigned to it. N_0 nodes that operate at high rate R, $N_0^{x_1}$ nodes that operate at r_1 and $N_0^{x_2}$ nodes that operate at r_2, Figure 3.5. We also assume that $r_1 < r_2$.

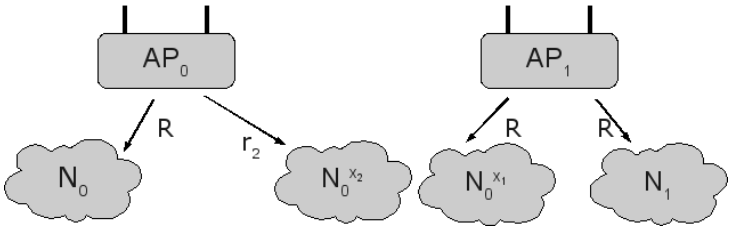

FIGURE 3.7: Mix of low-rate nodes. Handovers of the nodes that operate at r_1, $r_1 < r_2$.

***case a* (no handover):** In *case a*, where there is no handover, the long-term throughput of each access point is estimated by

$$X^a = \frac{p}{\frac{N_0}{N_0+N_0^{x1}+N_0^{x2}} \cdot T(p,R) + \frac{N_0^{x1}}{N_0+N_0^{x1}+N_0^{x2}} \cdot T(p,r_1) + \frac{N_0^{x2}}{N_0+N_0^{x1}+N_0^{x2}} \cdot T(p,r_2) + T(p,R)} . \tag{3.12}$$

The expected throughput of each node in N_0, N_0^{x1}, N_0^{x2} and N_1 is estimated by

$$X^a_{N_0} = X^a_{N_0^{x1}} = X^a_{N_0^{x2}} = \frac{1}{N_0 + N_0^{x1} + N_0^{x2}} X^a , \qquad X^a_{N_1} = \frac{1}{N_1} X^a$$

where X^a is estimated from (3.12).

***case b* (handover of low rate nodes):** When both low rate node sets, N_0^{x1} and N_0^{x2}, are handed over to N_1, Fig. 3.6, the estimated throughput of each access point is estimated by (3.6). The expected throughput of each node in N_0, N_0^{x1}, N_0^{x2} and N_1 is estimated by

$$X^a_{N_0} = \frac{1}{N_0} X^b , \qquad X^b_{N_0^{x1}} = X^b_{N_0^{x2}} = X^b_{N_1} = \frac{1}{N_1 + N_0^{x1} + N_0^{x2}} X^b$$

where X^b is estimated by (3.6). The inequalities

$$Gain_{AP_0} = \frac{X^b + \frac{N_0^{x1}+N_0^{x2}}{N_0^{x1}+N_0^{x2}+N_1} X^b}{X^a} > 1 \quad \text{and}$$

$$Gain_{AP_1} = \frac{\frac{N_1}{N_0^{x1}+N_0^{x2}+N_1} X^b}{X^a} > 1$$

are necessary conditions for *case b* to be beneficial for both access points. Similarly to the basic model, we notice that the handover is always beneficial for AP_0, because the inequality $Gain_{AP_0} > 1$ is always satisfied.

When only the N_0^{x1} are handed over to N_1, Fig. 3.7, the estimated throughput of each access point is

$$X^b = \frac{p}{\frac{N_0}{N_0+N_0^{x2}} \cdot T(p,R) + \frac{N_0^{x2}}{N_0+N_0^{x2}} \cdot T(p,r_2) + T(p,R)}$$

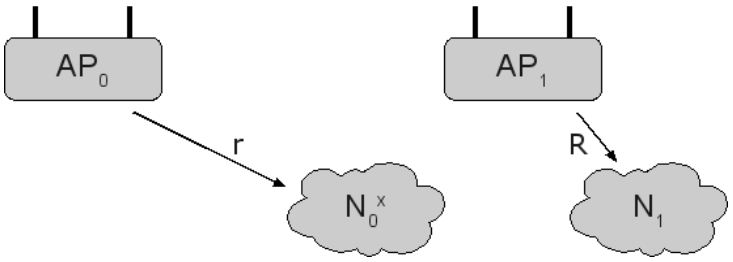

FIGURE 3.8: No N_0 nodes. No handovers performed (*case a*).

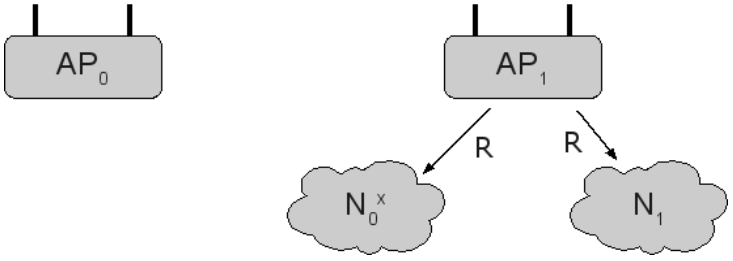

FIGURE 3.9: No N_0 nodes. Handovers performed (*case b*).

and the expected throughput of each node in N_0, $N_0^{x_2}$, $N_0^{x_1}$ and N_1 is

$$X^a_{N_0} = X^b_{N_0^{x_2}} = \frac{1}{N_0 + N_0^{x_2}} X^b \,, \qquad X^b_{N_0^{x_1}} = X^b_{N_1} = \frac{1}{N_1 + N_0^{x_1}} X^b$$

The gain inequalities are the following.

$$Gain_{AP_0} = \frac{X^b + \frac{N_0^{x_2}}{N_0^{x_2}+N_1} X^b}{X^a} > 1 \;\text{ and }\; Gain_{AP_1} = \frac{\frac{N_1}{N_0^{x_2}+N_1} X^b}{X^a} > 1 \,.$$

Depending on the actual low rates it is either beneficial to hand off all the nodes or only the nodes that operate at the lowest rate.

3.3.3 No N_0 nodes

We now assume that there are no nodes operating at high rate R for AP_0. The model for *case a* of this variation does not significantly change. By setting $N_0 = 0$, the formulas (3.4) and (3.5) still apply.

The model for *case b*, on the other hand, needs to be changed due to the fact that all AP_0's nodes are handed off to AP_1 and, as a result, there is now only one transmitter. The long-term throughput of each access point is

$$X^b = \frac{p}{T(p, R)} \,. \tag{3.13}$$

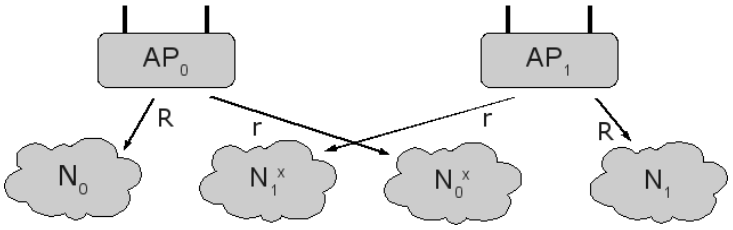

FIGURE 3.10: Swapping low rate nodes. No handovers performed (*case a*).

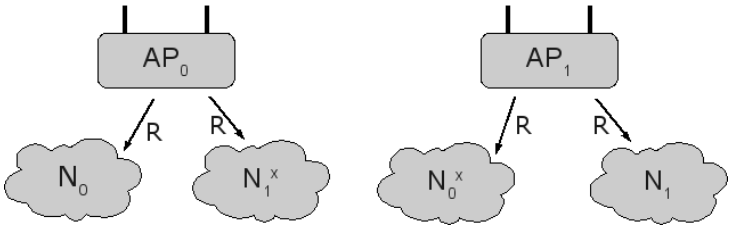

FIGURE 3.11: Swapping low rate nodes. Handovers performed (*case b*).

The formula (3.7) for the calculation of the estimated throughput of each node in N_0^x and N_1 also applies; however, X^b is now estimated by (3.13).

The necessary conditions for *case b* to be beneficial for the clients of both access points are the following.

$$Gain_{AP_0} = \frac{\frac{N_0^x}{N_0^x+N_1} X^b}{X^a} > 1 \text{ and } Gain_{AP_1} = \frac{\frac{N_1}{N_0^x+N_1} X^b}{X^a} > 1$$

As opposed to the basic scenario, the handover now is not always beneficial for the nodes of AP_0. The gain inequalities themselves can explain the reason. The handover is always beneficial for the basic scenario due to the fact that AP_0 used half of the channel for his high rate nodes N_0. Now that there are no N_0 nodes, there is a tradeoff for AP_0 between the performance degradation due to low rate transmissions and sharing the channel with the neighboring nodes. It is important to note, however, that the fact that in *case b* AP_1 does not contend for the shared medium tends to make handovers more beneficial.

3.3.4 Swapping low rate nodes

Next, we assume that, in addition to N_0^x, there is a set of AP_1 clients that operate at low rates, N_1^x, Fig. 3.10. These nodes operate at rate r and can potentially operate at rate R if they are handed off to AP_0.

When there is no handover, *case a*, the throughput of each access point is

$$X^a = \frac{p}{\frac{N_0}{N_0+N_0^x} \cdot T(p,R) + \frac{N_0^x}{N_0+N_0^x} \cdot T(p,r) + \frac{N_1}{N_1+N_1^x} \cdot T(p,R) + \frac{N_1^x}{N_1+N_1^x} \cdot T(p,r)} . \tag{3.14}$$

The expected throughput of each node in N_0, N_0^x, N_1 and N_1^x is

$$X_0^a = X_0^{x^a} = \frac{1}{N_0 + N_0^x} X^a \,, \qquad X_1^a = X_1^{x^a} = \frac{1}{N_1 + N_1^x} X^a \,,$$

where X^a is estimated from (3.14).

In the case of the mutual handover, Fig. 3.11, and since all nodes operate at high rate R, the throughput of each access point is estimated by (3.6). The expected throughput of each node in N_0, N_1^x, N_0^x and N_1 is

$$X_0^b = X_1^{x^b} = \frac{1}{N_0 + N_1^x} X^b \,, \qquad X_0^{x^b} = X_1^b = \frac{1}{N_0^x + N_1} X^b \,,$$

where X^b is estimated from (3.6). Hence, the gain inequalities are

$$Gain_{AP_0} = \frac{\frac{N_0}{N_0+N_1^x} X^b + \frac{N_0^x}{N_0^x+N_1} X^b}{X^a} > 1 \quad \text{and}$$

$$Gain_{AP_1} = \frac{\frac{N_1}{N_0^x+N_1} X^b + \frac{N_1^x}{N_0+N_1^x} X^b}{X^a} > 1$$

Swapping nodes increases the capacity of the wireless medium. Additionally, the wireless medium of each AP is shared among less nodes; comparing to the base scenario. As a result, we expect increased frequency of beneficial scenarios and increased gains.

3.4 Model Extensions

In this section we extend the basic throughput model to include capacity constraints outside of the wireless domain. We also investigate the application of priority mechanisms to differentiate the time AP_1 serves his clients and the guest clients.

3.4.1 Capacity Constraints

An important application of wireless LANs is to serve as an access network to wired networks, such as the Internet. It is not uncommon that the interconnection of a WLAN to the wired network is a bottleneck. This can be the case for DSL connections, whose speed depends on the distance of the subscriber to the provider's office where DSLAMs are located. Specifically, for distances larger than 3 Km, the capacity for ADSL+ falls below 8 Mbps, which is significantly lower than the maximum throughput supported by 802.11a/g. In this section we extend the throughput model to account for capacity constraints.

Consider that C_{AP_0} and C_{AP_1} is the wired capacity constraint of AP_0 and AP_1, respectively. First, we assume that $C_{AP_0} \leq C_{AP_1}$. The aggregate throughput of AP_0 is

$$X_{C_{AP_0}} = \min(C_{AP_0}, X) \ , \tag{3.15}$$

where X is the throughput that is estimated by the model in Section 3.2.2, for either the case of no handovers (3.4) or handovers (3.6).

If $C_{AP_0} < X$, then AP_0 uses less than its maximum share of the wireless channel, and AP_1 can potentially obtain a larger share. Hence, the aggregate throughput of AP_1 is

$$X_{C_{AP_1}} = \min(C_{AP_1}, a \cdot X_{C_{AP_0}}) \ ,$$

where factor $a \geq 1$ is the ratio of the number of frames sent by AP_1 over the number sent by AP_0, in the same time interval. In other words, if AP_0 is not constrained by C_{AP_0} then $a = 1$. If this is not the case, part of AP_0's share of the medium is available and can be used by AP_1. In both cases, factor a satisfies an equation which helps us come to a numerical solution to the respective linear equation system. When there are no handovers, factor a satisfies the equation

$$X^a_{C_{AP_0}} = \frac{p}{\frac{N_0}{N_0+N_0^x} \cdot T(p,R) + \frac{N_0^x}{N_0+N_0^x} \cdot T(p,r) + a \cdot T(p,R)} \ , \tag{3.16}$$

where $X^a_{C_{AP_0}}$ is given by (3.15) with $X \equiv X^a$. In the case of handovers, factor a satisfies

$$X^b_{C_{AP_0}} = \frac{p}{T(p,R) + a \cdot T(p,R)} \ , \tag{3.17}$$

where as before, $X^b_{C_{AP_0}}$ is given by (3.15) with $X \equiv X^b$.

If $C_{AP_1} < C_{AP_0}$, similar to the above, the aggregate throughput of AP_1 is

$$X_{C_{AP_1}} = \min(C_{AP_1}, X) \ , \tag{3.18}$$

where X is the throughput that is estimated by the model in Section 3.2.2, for either the case of no cooperation (3.4) or handovers (3.6). The aggregate throughput of AP_0 is

$$X_{C_{AP_0}} = \min(C_{AP_0}, a \cdot X_{C_{AP_1}}) \ ,$$

where factor $a \geq 1$ is the ratio of the number of frames sent by AP_0 over the number sent by AP_1, in the same time interval. Similarly, in the case of no handovers, factor a satisfies

$$X^a_{C_{AP_1}} = \frac{p}{a \cdot (\frac{N_0}{N_0+N_0^x} \cdot T(p,R) + \frac{N_0^x}{N_0+N_0^x} \cdot T(p,r)) + T(p,R)} \ , \tag{3.19}$$

where $X^a_{C_{AP_1}}$ is given by (3.18) with $X \equiv X^a$. In the case of handovers, factor a satisfies

$$X^b_{C_{AP_1}} = \frac{p}{a \cdot T(p,R) + T(p,R)} \ , \tag{3.20}$$

where as before, $X^b_{C_{AP_1}}$ is given by (3.18) with $X \equiv X^b$.

By applying the respective values of $X_{C_{AP_0}}$ and $X_{C_{AP_1}}$, the conditions that predict when the handovers are beneficial for each access point when the objective is throughput maximization ($u(x) = x$) are

$$Gain_{AP_0} = \frac{X^b_{C_{AP_0}} + \frac{N_0^x}{N_0^x+N_1} X^b_{C_{AP_1}}}{X^a_{C_{AP_0}}} > 1 \ \text{ and } \ Gain_{AP_1} = \frac{\frac{N_1}{N_0^x+N_1} X^b_{C_{AP_1}}}{X^a_{C_{AP_1}}} > 1 \tag{3.21}$$

When both capacity constraints, C_{AP_0} and C_{AP_1} are lower than the throughput X^a given by (3.4), then the handovers cannot be beneficial. Moreover, when both throughput constraints are greater than the throughput X^b given by (3.6), then the constraints do not affect the handovers, and the gains can be estimated by the model in Section 3.2.2.

3.4.2 Unsaturated Conditions

Next, we investigate the case of unsaturated conditions where each access points transmits traffic at a constant bit rate lower than the saturated conditions. Consider that R_{AP_0} and R_{AP_1} is the bit rate in application layer of AP_0 and AP_1, respectively.

We assume that $R_{AP_0} \leq R_{AP_1}$. The modeling framework for the complementary assumptions can be similarly deduced. The aggregate throughput of AP_0 is

$$X_{R_{AP_0}} = \min(R_{AP_0}, X) \ , \tag{3.22}$$

where X is the throughput estimated by the model in Section 3.2.2, for either the case of no handovers (3.4) or handovers (3.6).

If $R_{AP_0} < X$, then AP_0 uses less than its maximum share of the wireless channel, and AP_1 can potentially obtain a larger share. Hence, the aggregate throughput of AP_1 is

$$X_{R_{AP_1}} = \min(R_{AP_1}, a \cdot X_{R_{AP_0}}) \ ,$$

where factor $a \geq 1$ is the ratio of the number of frames sent by AP_1 over the number sent by AP_0, in the same time interval.

In the case of no handovers, factor a satisfies the equation (3.16) where $X^a_{C_{AP_0}} \equiv X^a_{R_{AP_0}}$ is given by (3.22) with $X \equiv X^a$. In case of handovers, factor a satisfies (3.17) where as before, $X^b_{C_{AP_0}} \equiv X^a_{R_{AP_0}}$ is given by (3.22) where $X \equiv X^b$.

The analysis suggests that the modeling framework is similar to the case of capacity constraints.

3.4.3 Client Differentiation

The basic model assumes the handed-over nodes are treated as equal clients by their new host. Equation (3.8) shows that the gain for AP_0 is expected to be much higher than the gain of AP_1 as the clients of the former use part of the resources of the latter. This is validated in the analytical experiments in Section 3.5. On the other hand, AP_1 can control the way the gain is shared between his clients and the clients of AP_0. In a nutshell, AP_1 can use two priority queues; one for his clients and one for the guest clients which belong to AP_0. This can be supported by standards such as IEEE 802.11e [MCH+03].

Consider that AP_1 sends $a \geq 1$ frames to its clients for every frame it sends to the guest clients. The gain for each access point, assuming the objective is throughput maximization, are expressed by the following inequalities

$$Gain_{AP_0} = \frac{X^b + \frac{1}{a+1}X^b}{X^a} > 1 \text{ and } Gain_{AP_1} = \frac{\frac{a}{a+1}X^b}{X^a} > 1$$

where X^a and X^b are given by (3.4) and (3.6) respectively.

We make the remark that the gains do not depend on the number of N_0, N_0^x or N_1 nodes. The increased gain of AP_1 balances the gains between the access points by increasing the gain of AP_1 and decreasing the gain of AP_0. As a result, client differentiation turns into beneficial many cases that yield negative gains to AP_1 in the base scenario.

AP_1 has incentives to increase the factor a since this would maximize the performance improvements of its clients. We notice that when $a \to \infty$ both access points have equal gains. This leads the low rate nodes to starvation. However, if the low rate nodes have the ability to choose access points, then AP_1 needs to offer them an improved performance in order to keep them as guest clients.

3.5 Analytical Investigations

In this section we present a series of analytical experiments that aim to identify the performance gains of handovers in different scenarios. First, we describe the node diversity model. Next, we

present the normalized gain; the metric with which we evaluate the handovers in long-term.

The protocol overhead is important to precisely estimate the average throughput. A zero overhead, as assumed in (3.3), provides an upper bound of the throughput gains. For the analytical and simulation experiments we consider an overhead model based on the theoretical maximum throughput estimation in [JPS03]. The overhead model is described in detail in Appendix A.1.

3.5.1 Node Density Model

The node density of each access point depends on its environment. Therefore, there are hotspots when the access points serve many nodes and other spots where they serve few nodes. For the experiments presented in this section, we require a node density model that captures a wide range of environments.

We assume that the number of the nodes of each set follows a normal distribution. The mean of each distribution is equal to $\frac{\mu}{n}$ where n is the number of node subsets in each access point and the variance is equal to σ^2. For all the following experiments, apart from the experiments presented in Section 3.5.3.2, we assume that $\mu = 6$ and $\sigma^2 = 2$. For example, in the baseline scenario the sets N_0 and N_0^x follow a normal distribution where the mean is equal to $\frac{\mu}{n} = \frac{6}{2} = 3$. In Section 3.5.3.2, we investigate the effects of these parameters.

3.5.2 Evaluation Metric

In order to evaluate the long-term gain we use the following metric that we refer to as *normalized gain*.

$$NormGain_{AP_i} = \frac{1}{N}\sum_{k=1}^{N} x_{i_k}\,, \quad \text{where} \quad x_i = \begin{cases} Gain_{AP_i} & \text{: handovers performed} \\ 1 & \text{: otherwise} \end{cases}$$

When the model predicts that $Gain_{AP_i} > 1$ for all access points then the handovers are performed and each access point has a throughput gain. When the model predicts that the handovers will not be beneficial then no handover is performed and the access points have no gain. The normalized gain is an average of beneficial scenarios where the gain is positive and non-beneficial scenarios where there is no gain. Therefore, this metric can capture both the frequency and the gains of a beneficial scenario. Additionally, this metric captures the effects of potential false positives and false negatives. All normalized gains in Section 3.5.3 are calculated using $N = 2000$.

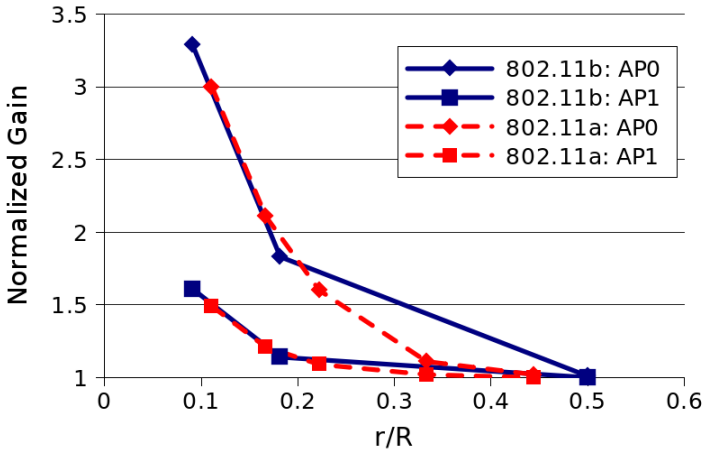

FIGURE 3.12: Base scenario in 802.11b and 802.11a.

3.5.3 Analytical Investigations

In this section we perform a series of analytical experiments in order to identify the trends and trade-offs of the proposed handovers.

3.5.3.1 Base Scenario

Figure 3.12 depicts the normalized gain for the base scenario in 802.11b and 802.11a for various values of the low rate r. The rate R is equal to the highest rate supported by each protocol, 11 Mbps and 54 Mbps respectively. We have observed similar behavior in both protocols. The small differences are due to differences in their overhead. Observe that there are significant long-term performance improvements when the rate r is low; less or equal to 2 Mbps and 12 Mbps in 802.11b and 802.11a respectively. For higher rates, r, the beneficial scenarios are a few. However, the model predicts when the handover is not beneficial and, as a result, the normalized gain is always positive.

Figure 3.13 depicts the line defined by (3.9) for 802.11b and its supported rates. The threshold c is adjusted to the overhead model defined in Appendix A.1. The x and y axis shows the number of AP_1 and AP_0 nodes, respectively. The slope of each line is given by c. Every N_0, N_0^x, N_1 combination that is below each line can benefit with the handover of low-rate nodes. The area below each line provides a visual estimation of the frequency of the appearance of a beneficial scenario, across all possible scenarios that correspond to all $N0, Nx, N1$ combinations. The figure shows that when the low rate is 1 Mbps beneficial scenarios are highly likely. When the low rate is 2 Mbps the beneficial area is reduced to half. When the low rate is 5.5 Mbps the beneficial area is very small, and beneficial handovers for both access points in this case are infrequent.

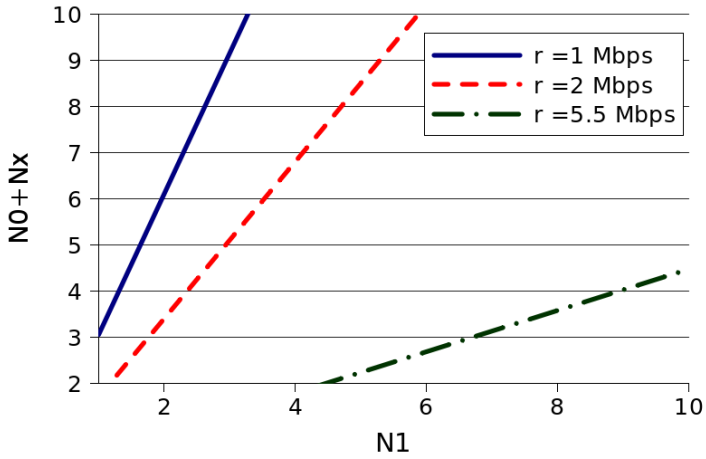

FIGURE 3.13: Threshold c in 802.11b. All areas below each line refer to beneficial scenarios.

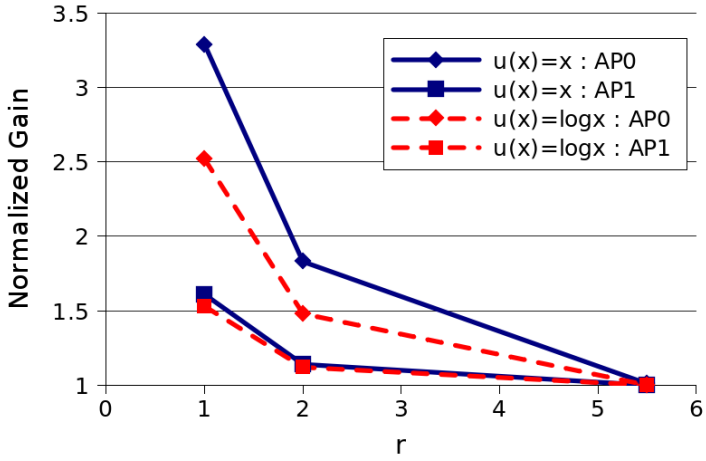

FIGURE 3.14: Base scenario in 802.11b for different objectives.

Finally, Figure 3.14 shows the normalized gain for different objectives; throughput maximization and fairness. It is important that the frequency of beneficial scenarios is similar for both objectives, although in the later the value of throughput is much less. This happens because is the vast majority of the beneficial scenarios the performance is improved for all the clients. On the other hand, the value of throughput affects the normalized gain which is reduced. We note that this reduction is more significant for AP_0 as it achieves higher throughputs that now value less.

3.5.3.2 Effects of Density Model

Next, we experiment on the effects of the node density model parameters on the normalized gain. Both experiments that follow refer to the base scenario in 802.11b where $r = 1$ Mbps.

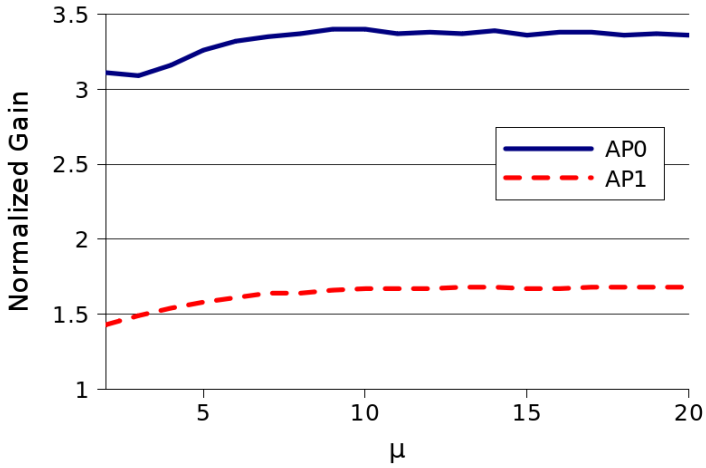

FIGURE 3.15: Experimenting on the *mean* of the node density model.

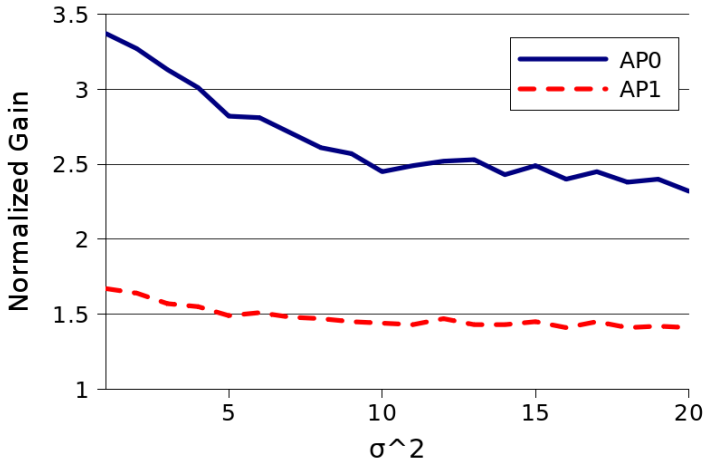

FIGURE 3.16: Experimenting on the *variance* of the node density model.

In the experiment presented in Figure 3.15 the variance is constant and equal to 2 similarly with the previous experiments. The x-axis is the mean, μ, of the normal distribution as described in Section 3.5.1. We observe that the normalized gain is slightly increasing as the average node density increases. The experiment shown in Figure 3.16 experiments on the variance. The mean is constant and equal to 6. The normalized gain is decreasing as the variance increases. However, variance affects mainly the gains of AP_0.

Concluding, we can safely assume that the basic trends of the handovers are valid is either dense or sparse scenarios.

3.5.3.3 Different Topologies

Figure 3.17 depicts the results for the three-access-point scenario in 802.11b. The performance gains are higher compared to the base scenario, Figure 3.12, since the low rate nodes are handed

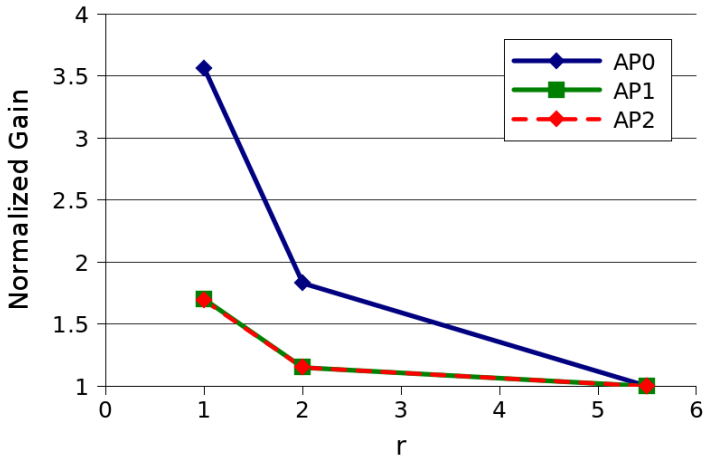

FIGURE 3.17: Three access points in 802.11b.

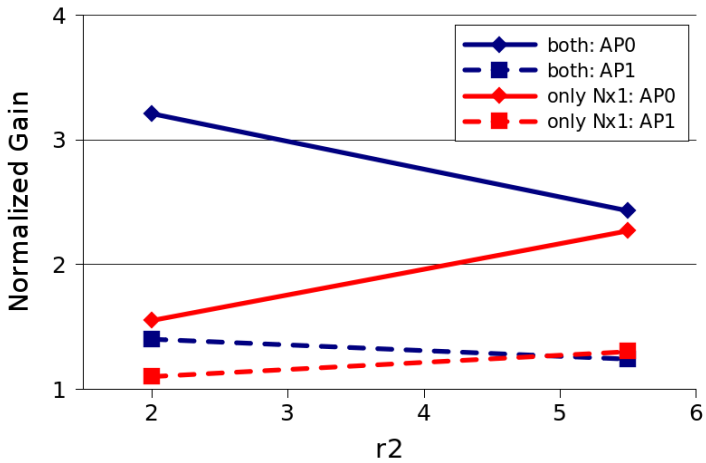

FIGURE 3.18: Mix of low rate nodes where $r_1 = 1$ Mbps in 802.11b.

over and served by two access points. Moreover, all APs benefits by the elimination of the low rate transmissions.

Next, in Figure 3.18 we show the gains for the scenario where two low-rate node-sets exists in 802.11b. We assume that the first set of low rate nodes operates at $r_1 = 1$ Mbps while the other set operates at either $r_2 = 2$ Mbps or $r_2 = 5.5$ Mbps. We investigate whether it is better to hand over all low rate nodes or only the set that operates at the lowest rate, r_1. The best for AP_1 is to accept all the nodes when r_2 is small and to accept only the nodes that operate at $r_1 = 1$ Mbps when r_2 is relatively high. It is clear in Figure 3.18 that the performance gain for AP_1 follows this trend. For AP_0 although it is always better to pass all his low rate clients to the neighboring AP.

Figure 3.19 depicts the simplified scenario where there are no clients in the N_0 set. Although the handovers are not always beneficial for AP_0 we can see that the long-term performance gains are much better than the basic scenario. This occurs because all resources are used by

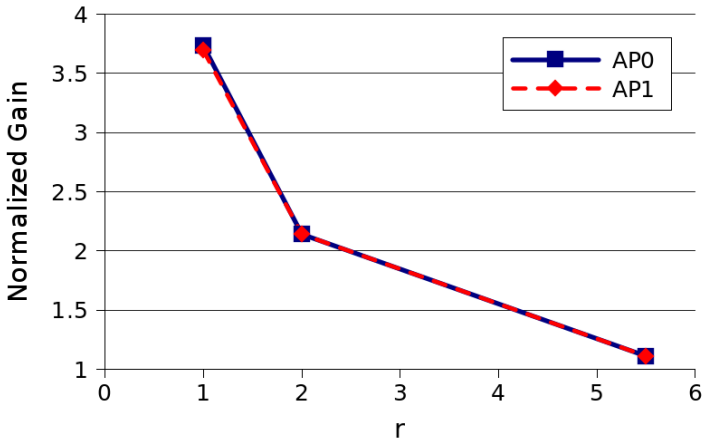

FIGURE 3.19: No N_0 nodes in 802.11b.

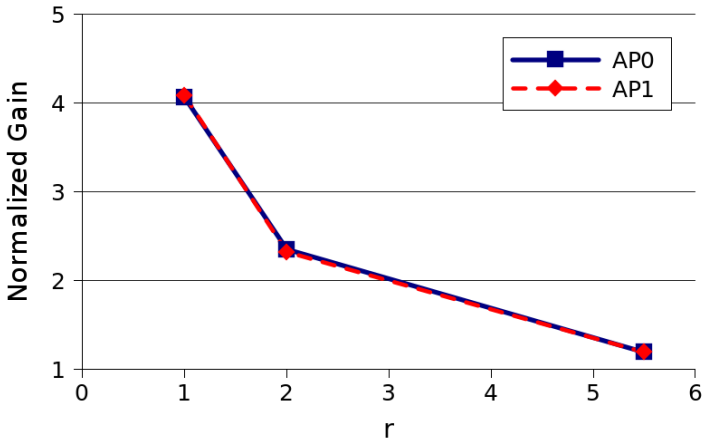

FIGURE 3.20: Swapping low rate nodes in 802.11b.

AP_1. The clients of AP_1 achieve double throughput compared to the scenario where the N_0 set has at least one client.

Figure 3.20 shows the symmetric scenario where the access points swap low rate nodes. The aggregate capacity is increased due to the elimination of the low rate transmissions. Additionally, both APs serve guest clients and have some of their clients served by the neighboring network. Hence, swapping nodes improves the performance gains and balances them between the two parties.

3.5.3.4 Capacity Constraints and Client Differentiation

The following figures investigate the capacity constraints on the gains of the handovers. The investigations are performed in 802.11a where the low rate is equal to 6 Mbps.

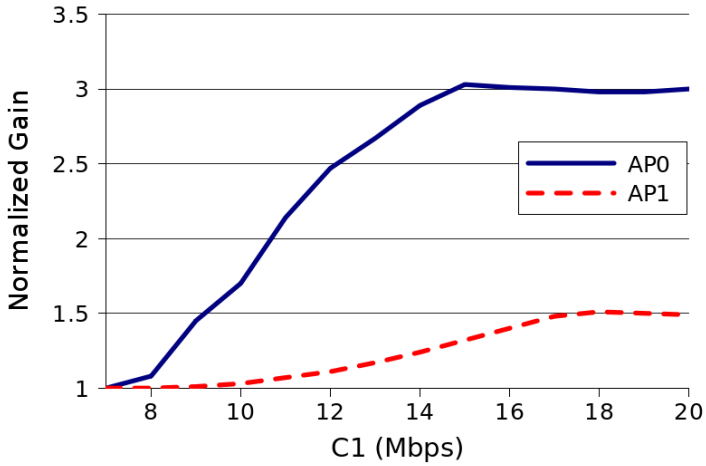

FIGURE 3.21: Capacity constraints in 802.11a where $r = 6$ Mbps and $C_0 = 54$ Mbps.

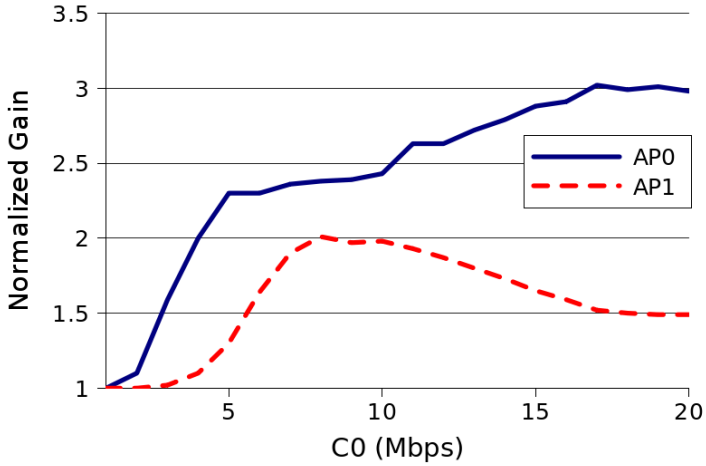

FIGURE 3.22: Capacity constraints in 802.11a where $r = 6$ Mbps and $C_1 = 54$ Mbps.

In Figure 3.21 the bottleneck for AP_0 is the wireless link. However, AP_1 is bottlenecked by a wired link whose capacity is the x-axis, C_1. As expected, there are three clear zones in the normalized gain. When C_1 is very low, thus highly restrictive, there are no gains. When C_1 is higher than 18 Mbps then the wired link is not a bottleneck. Hence, the gains for this scenario are identical to the main model. Figure 3.22 depicts the symmetric scenario where there is no constraint for AP_0. The x-axis is the constraint for AP_1. There is a similar behavior for the two edge zones. The behavior of the gain in the middle zone is more complicated, since the increase of the capacity of AP_0 has two effects. The first is that the low rate clients transmit more frames when handovers are not performed which tends to make the handovers more beneficial. The second is that AP_1 transmits less traffic, decreasing its capability to serve guest clients, which tends to make the handovers less beneficial. The behavior of the gain in the middle zone is the result of these two effects. Additionally, in both scenarios that the non-constraint access point makes use of the unused medium of the constrained access point.

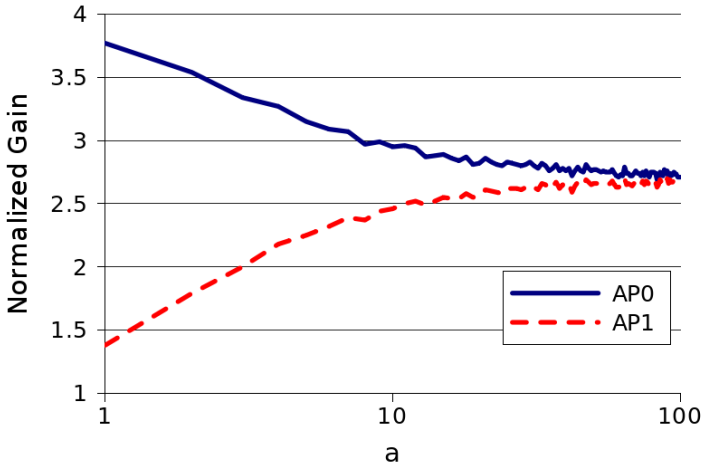

FIGURE 3.23: Client differentiation by AP_1 in 802.11b where $r = 1$ Mbps.

AP_1 can control how the gain is shared between the parties by applying priorities between its clients and the guest clients. Figure 3.23 shows the normalized gain when AP_1 sends a frames to its clients for every frame it sends to the handed-over clients. The experiments were performed in 802.11b and $r = 1$ Mbps. It is clear that as a increases the gains are balanced out between the access points. Additionally, beneficial scenarios that lead to handovers become more frequent.

3.6 Simulation and Experimental Evaluation

The accuracy of the analytical framework is evaluated and validated through simulations and experiments on real test-bed. Simulation experiments evaluate the model in dense networks that consist of many nodes, whereas the experiments on real test-bed provide a more accurate comparison of the model with an actual network.

3.6.1 Simulations

First, we present simulation experiments based on NS-2, to validate the throughput model and verify that it can accurately estimate the throughput gains that are achieved through handovers. The default version of NS-2 does not support multiple rates for transmissions between one transmitter and multiple receivers. Hence, we extended NS-2 to support multiple rates by adapting the transmission rate according to the signal strength of the last received frame. The overhead of a transmission is expected to be different in NS-2, since the model does not account for collisions; this simplification is expected to result in lower gains than those predicted by the model.

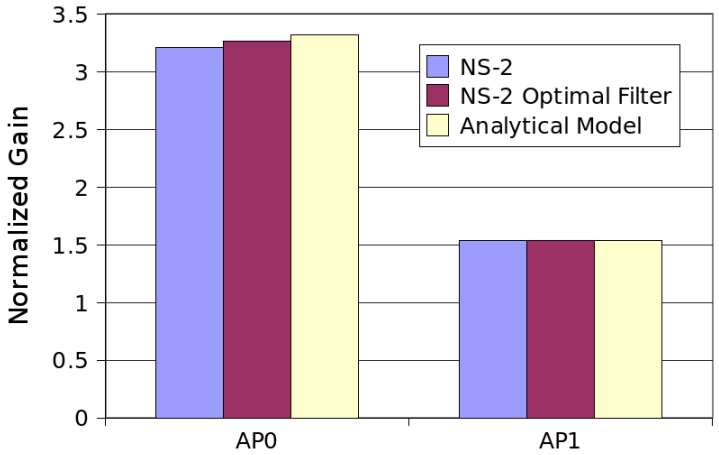

FIGURE 3.24: Comparison of model estimations and simulations.

We simulate the 802.11b version of the basic scenario presented in Section 3.2. The low rate, r, is 1 Mbps and the high rate, R is set to the maximum available rate supported by the protocol, namely 11 Mbps. The presented results show the normalized gain over all the potential scenarios for various node sets, N_0, N_0^x and N_1, assuming that each AP serves up to 10 nodes. The experiments used UDP traffic, and each run had duration 15 seconds. The column named *Analytical Model* in Figure 4.19 refers to the analytical results of the experiment as estimated by the proposed model.

The simulations indicate that there is no single threshold that separates the beneficial scenarios from the non-beneficial ones. If the constant c predicted by the model is used for accepting or rejecting handovers, there are 0.4% false positives and 2% false negatives. The results show that the handover admission threshold used by AP_1 is conservative as it produces a very minimal number false positives in exchange with false negatives. However, the gain of the false negative scenarios is low; less than 5% in the vast majority of the scenarios.

In Figure 3.24 the column *NS-2 Optimal Filter* refers to a theoretical optimum filter that perfectly predicts the beneficial and non-beneficial scenarios. This figure shows that the handover policy based on the threshold c (in figure named *NS-2*) performs extremely well, giving a normalized gain for AP_1 which is within 0.01% of the maximum gain, which is achieved by the theoretical optimal filter. The normalized gain for AP_0 is within 4% of the theoretical maximum gain. The accuracy of the model is also verified as its estimations are very close to the results of the simulation experiments.

Finally, the simulations show that the effects of the collision simplification on the normalized gains are insignificant. This was expected because in the downlink direction only two access points contend for channel access.

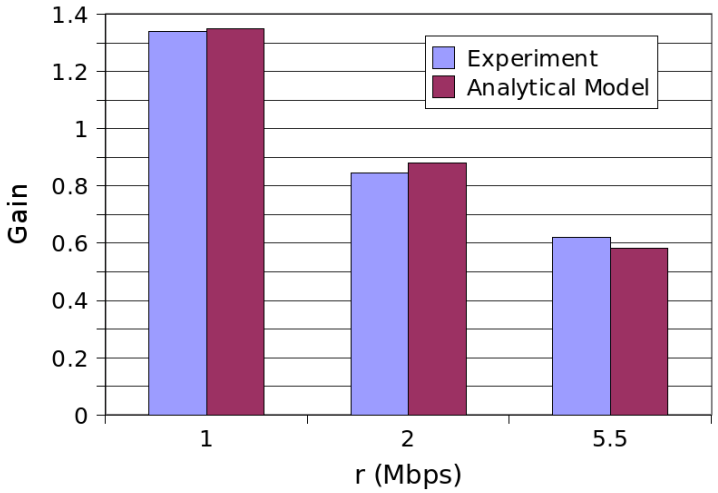

FIGURE 3.25: Comparison of model estimations and experiments.

3.6.2 Experiments on Real Test-bed

Next we evaluate the accuracy of the modeling framework on a real test-bed. The experiments performed refer to the basic scenario presented in Section 3.2 in 802.11b where each node-set consists of one node ($N_0 = N_0^x = N_1 = 1$). Hence, we used three wireless clients and two Cisco's Aironet 1240AG access points [Sys]. The low rate, r, was manually set to 1, 2 and 5.5 Mbps through the driver of wireless adapter of the low rate client. The high rate, R was set to the maximum available rate supported by the protocol, namely 11 Mbps. The experiments used UDP traffic, and each run had duration 60 seconds.

Figure 3.25 shows the average gain of the N_1 client over multiple instances of the same experiment in comparison to estimations of the model. The average gain of experiments and the model estimations are very close. Additionally, there are neither false positives nor false negatives in the predictions whether the handover is beneficial or not. Therefore, in this scenario the accuracy of the model is verified.

3.7 Implementation

The experiments show that it is feasible for wireless networks administrators to benefit from handovers by using the analytical model to identify when the performance incentives arise. In this section we discuss the prototype implementation of an automated system that performs handovers according to the predictions of the analytical model.

The handover process followed by AP_1 is being depicted in Fig. 3.26. As it is shown there, the AP_1 is performing passive measurements for nearby stations to examine the existence of low rate transmissions and then it can extract from the measurements the needed information to

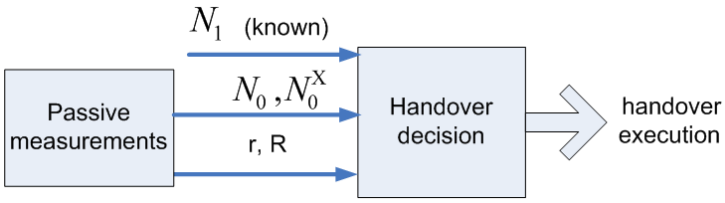

FIGURE 3.26: Handover process in AP_1.

compute (3.9) to take a decision if it will request the handover of the low rate nodes. If (3.9) is satisfied, then AP_1 will continue to the execution of the handover and communicate with AP_0 for the rest of the handover process.

The handover acceptance policy requires that the access points know the number of connected nodes and their rates. Assuming that there are no hidden nodes, this information is easy to obtain by monitoring the neighboring traffic. The access point can count unique MAC addresses and extract the rates from their PLCP header. Alternatively, the neighboring access points can directly communicate and exchange all the information required. This approach provides a solution in the case of hidden nodes. However, issues arise if malicious access points may provide false information. Additionally, the access point needs to estimate the rate that the low rate nodes would operate at, if handovers are performed. Measuring the received signal strength of the frames the low rate nodes transmit can be useful for this estimation.

The handover process for the implementation of the algorithm is shown in Fig. 3.27. The number of the connected nodes to AP_1 is of course known to AP_1. The passive measurement module performs the local measurements at a mesh node's wireless interfaces. These are measurements regarding physical layer measurements of the link quality, such as the signal-to-noise ratio and frame loss ratio, link load measurements, such as the channel utilization and number of interfering wireless interfaces, and higher-level performance measurements, such as achievable throughput and packet delay. From these measurements the AP_1 can extract information about the neighboring nodes and extract their MAC addresses and their transmission rates. Then equation (3.9) is applied. If it is satisfied, the handover is initiated. Upon recognition of a beneficial scenario, there are two approaches for the handovers themselves. First, the access points can directly communicate, exchange the required information and execute the handovers. Alternatively, AP_0 does not need participate. Whenever AP_1 recognizes that it can serve neighboring nodes at higher rates with gains for its clients, it can allow the low rate nodes to associate with it. The low rate nodes, by default, choose the available access point with the highest signal quality in order to communicate at higher rates.

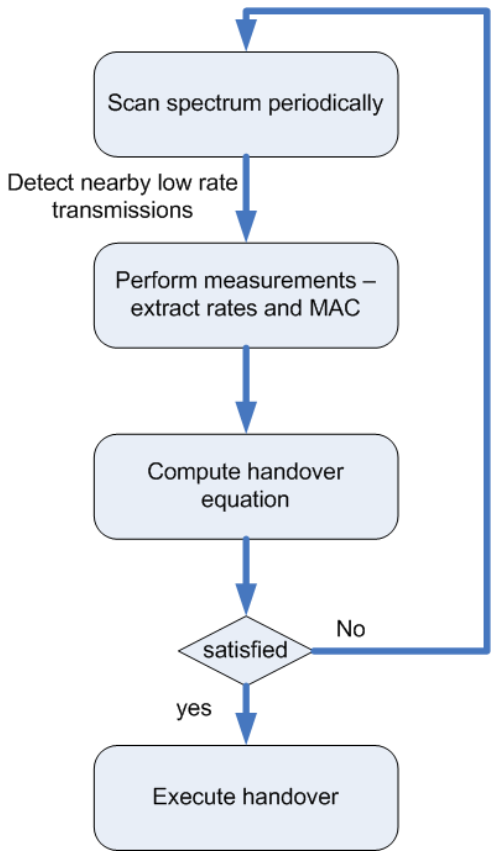

FIGURE 3.27: Implementation of handover process.

3.8 Conclusions

We analyzed scenarios where the cooperation between public/home wireless network administrators is motivated solely by the performance improvement for their clients. Using an analytical throughput model we computed the throughput gains for all parties, when low rate users are handed-off to the closer access point. Moreover, the analytical model suggests a simple acceptance policy for deciding when handovers are beneficial. Additionally, we extended the model to include wired capacity constraints, e.g., from ADSL connections. We also investigate the application of client differentiation mechanisms which allows to control the sharing of the handover gains among the involved access points.

Finally, the analytical model was compared with simulation results and real experiments, which verify the accuracy of the model. Based on the simulation results we conclude that the throughput model can accurately predict when such incentives arise; with a small number of false positives, that have insignificant effect to the long-term gain.

Chapter 4

Cooperation Incentives in Wireless Mesh Networks

4.1 Incentives in WMNs

Due to their multi-hop nature, in wireless mesh networks low rate links create bottlenecks that degrade the end-to-end performance. Moreover, the performance anomaly of 802.11 arises in links that operate at different rates in the same channel. In this chapter we investigate the incentives for mesh node sharing between different WMN operators. Such cooperation can significantly improve the end-to-end throughput of both WMNs. Hence, the cooperation is motivated due *solely* to the improved performance that cooperation yields for *both* wireless networks.

We investigate both the case where there is a limited number of channels available, forcing mesh nodes to operate in the same channel, and the case where there are many orthogonal channels available and their usage is constrained solely by the number of radios in each mesh node. For 802.11b/g that operates in the 2.4 GHz band, it is common to have more than three transmitters on the same channel within range of each other [AJSS05]. Hence, the three orthogonal channels available in 802.11b/g are not sufficient to assign orthogonal channels to all interfering links in dense wireless deployments. The second case, namely the existence of sufficient orthogonal channels (four channels or more), is applicable to 802.11a that operates in the 5 GHz band [KV06]. In this case, usage of the available orthogonal channels can be constrained by the number of radios available in each mesh node. For this reason, we investigate the case of one, two, and three radio mesh nodes. We find that, even when there is no performance degradation due to the co-existence of low and high-rate transmitters, significant performance improvements can still be achieved by replacing a low-rate link with two high-rate links.

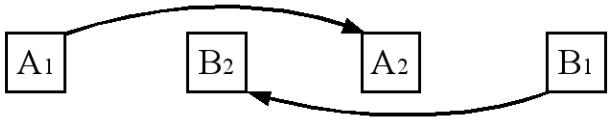

FIGURE 4.1: No Mesh Node Sharing (*Case a*).

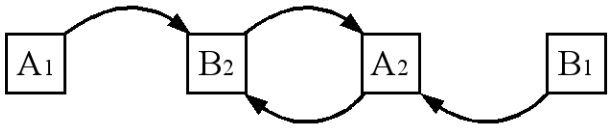

FIGURE 4.2: Mesh Node Sharing (*Case b*).

The contributions of this investigation include the following:

- Analysis of a simple model for estimating the end-to-end throughput in multi-hop wireless mesh networks, that accounts for rate diversity.
- Application of the above model to identify and quantify the improved performance that can be achieved with the cooperation of mesh networks.
- The analysis considers the case where the same channel is used by all mesh nodes, the case where many orthogonal channels are available and their usage is limited by the number of radios in each mesh node, and when there exist capacity constraints due to links outside the wireless mesh network.
- Validation of the analytical model by comparing the gains it estimates, with simulation results.

4.2 Throughput Model

Consider two mesh networks, A and B, and an overlapping part of these networks that consists of a sequence of four nodes, A_1, B_2, A_2, and B_1. Network A has traffic originating from node A_1 and destined to node A_2, while B has traffic originating from node B_1 and destined to node B_2. When the two networks do not cooperate, which will be referred to as *case a* (Figure 4.1), there are two flows from A_1 to A_2, and from B_1 to B_2. On the other hand, when the two mesh networks cooperate (Figure 4.2), nodes B_2 and A_2 act as relays for the two traffic flows belonging to A and B, respectively. As a result, the end-to-end flow of network A traverses two hops, A_1B_2 and B_2A_2, and that of network B traverses two hops, B_1A_2 and A_2B_2; we will refer to this scenario as *case b*. Observe that there are two transmitters contending for the wireless channel in *case a*, while there are four transmitters in *case b*.

Gain is the metric we use in order to evaluate when the cooperation of the wireless mesh networks (*case b*) is beneficial for both networks. It is defined as the ratio of the long-term end-to-end throughput, X, of a mesh network in *case b*, over that of *case a*.

$$Gain_k = \frac{X_k^b}{X_k^a}\,, \tag{4.1}$$

where k is either A or B. $Gain_k > 1$ indicates that for network k the cooperation is beneficial, i.e. the network achieves higher end-to-end throughput compared to the throughput it achieves when there is no cooperation. When $Gain_k > 1$ for both $k = A, B$, then cooperation is beneficial for both networks.

We denote d_{ij} the distance between the nodes i and j, and assume that all nodes are in the same contention area. We also assume that there is a rate adaptation mechanism, and consider the function $R(d)$ that gives the rate for different distances d. This transmission rate, in general, depends on the transmission power, the antenna gains, the path loss, and the receiver's sensitivity thresholds. For the analytical experiments in Section 4.4, we consider a specific path loss model. The analytical throughput model presented in this section can consider any rate function.

The proposed throughput model considers the function $T(p, R)$, which denotes the expected duration for the transmission of a frame with payload size p, when the link layer transmission rate is R. If we disregard all overheads, this function is given by

$$T(p, R) = \frac{p}{R}\,. \tag{4.2}$$

The last expression captures a key property of wireless networks, namely that the duration of a packet transmission is higher for nodes with a smaller transmission rate. In Appendix A.1 we present an expression for $T(p, R)$ that includes all protocol overheads.

Next we present the analytical throughput model for Figs. 4.1 and 4.2, for single and multiple channel scenarios.

4.3 Single Channel

First, we assume that every mesh node has a single radio that operates on the same channel. This scenario can be the case for dense networks, where the number of orthogonal channels is limited, e.g. for 802.11b wireless networks operating in the 2.4 GHz band.

***Case a* (no cooperation):** In this case, Figure 4.1, the mesh networks do not cooperate

but share the same wireless channel. Assuming a MAC layer protocol that provides long-term fairness, e.g. 802.11's DCF, the long-term throughput of each mesh network can be approximated by

$$X^a = \frac{p}{T(p, R(d_{A_1A_2})) + T(p, R(d_{B_1B_2}))} , \tag{4.3}$$

where p is the frame payload size, and $T(\cdot)$ is given by (4.2). The above expression approximates the shared wireless channel as a polling or round robin system, where each node A_1 and B_2 transmits one frame in consecutive rounds.

***Case b* (cooperation):** In this case, Figure 4.2, a frame is forwarded across two hops to reach the destination. We now have four contending transmitters, A_1, A_2, B_1, and B_2, and the long-term end-to-end throughput of each mesh network can be approximated by

$$X^b = \frac{p}{T(p, R(d_{A_1B_2})) + 2 \cdot T(p, R(d_{B_2A_2})) + T(p, R(d_{B_1A_2}))} , \tag{4.4}$$

where, for simplicity, we have assumed that $R(d_{ij}) = R(d_{ji})$. Substituting the above expressions for X^a and X^b in (4.1), we obtain the following inequality that is necessary for the cooperation to be beneficial for both mesh networks.

$$\frac{T(p, R(d_{A_1A_2})) + T(p, R(d_{B_1B_2}))}{T(p, R(d_{A_1B_2})) + 2 \cdot T(p, R(d_{B_2A_2})) + T(p, R(d_{B_1A_2}))} > 1 .$$

The last equation captures a key trade-off in the scenario considered in this section: Cooperation can allow transmissions at higher rates, since the distances $d_{A_1B_2}, d_{B_2A_2}, d_{B_1A_1}$ are smaller than $d_{A_1A_2}$ and $d_{B_1B_2}$, but two transmissions are required for the end-to-end forwarding of each frame, compared to a single transmission in the case of no cooperation. Positive incentives for cooperation will exist if the improvements due to the higher transmission rates outweigh the overhead of forwarding each frame twice. Finally, note that the gain for both mesh networks is the same, since they share the same channel.

4.3.1 Multiple Channels

Next we assume that a sufficient number of orthogonal channels are available, so that every link can operate on a different channel. This scenario requires up to four available orthogonal channels and it applies to 802.11a networks operating in the 5 GHz band [KV06]. Although there can be many available channels, the number of radios available in each mesh node can be a limiting factor for their usage. For this reason, we next investigate the cases where each mesh node has one, two, or three radios.

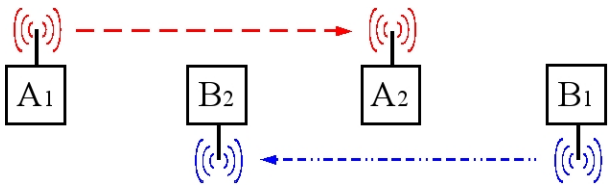

FIGURE 4.3: Multi-channel, 1-radio nodes, no mesh node sharing.

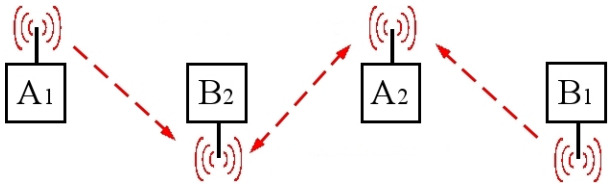

FIGURE 4.4: Multi-channel, 1-radio nodes, mesh node sharing.

***Case a* (no mesh node sharing):** When the mesh networks do not cooperate, links A_1A_2 and B_1B_2 can operate on a different channel, Figure 4.3. Hence, the two networks do not contend with each other. The long-term throughput for each mesh network is approximated by

$$X_A^a = \frac{p}{T(p, R(d_{A_1A_2}))} \ , \ \ X_B^a = \frac{p}{T(p, R(d_{B_1B_2}))} \ . \tag{4.5}$$

The above equations are independent of the number of radios in each mesh node, since each mesh node has a link to only one neighboring node.

***Case b* (mesh node sharing):** In this case the contention for channel access depends on the number of radios available in each mesh node, and the analytical throughput expression will be different for a different number of radios. Next we consider the case of one, two, and three radio mesh nodes.

Single-radio nodes: The case of cooperation for single-radio nodes is similar to the single channel scenario presented in the previous section. Therefore, the end-to-end throughput is given by (4.4). This scenario favors cooperation less than the scenario where all nodes operate on the same channel, since without cooperation the two mesh networks can operate on different orthogonal channels, Figure 4.3, which reduces contention. The experiments in Section 4.4 indicate that there can still be cases where cooperation is beneficial, but the gains are very small.

Two-radio nodes: This is the common case for wireless mesh devices, which typically have three radios, one for client access and the remaining two for mesh node connectivity. Now, links A_1B_2, B_2A_2, and A_2B_1 can operate on a different channel, Figure 4.6. There is a single flow on links A_1B_2 and A_2B_1, and two flows with opposite direction on link B_2A_2; hence, in the latter link there are two transmitters, A_2 and B_2, which contend for the same channel.

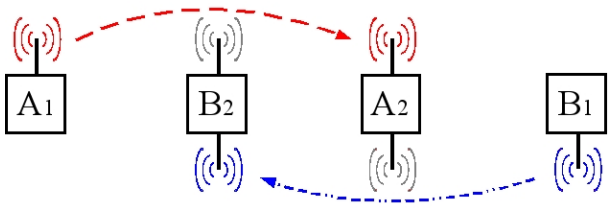

FIGURE 4.5: Multi-channel, 2-radio nodes, no mesh node sharing.

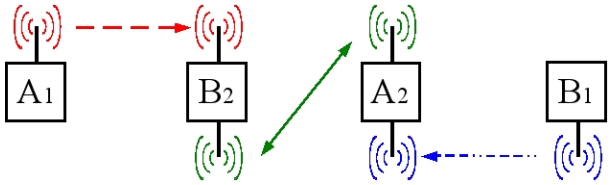

FIGURE 4.6: Multi-channel, 2-radio nodes, mesh node sharing.

The maximum throughput for each of the two flows traversing the middle link B_2A_2 can be approximated by

$$X^b_{B_2A_2} = \frac{p}{2 \cdot T(p, R(d_{B_2A_2}))}\,, \tag{4.6}$$

where as before we have assumed that $R(d_{ij}) = R(d_{ji})$. The maximum throughput on links A_1B_2 and B_1A_2 can be approximated by

$$X^b_{A_1B_2} = \frac{p}{T(p, R(d_{A_1B_2}))}\,, \tag{4.7}$$

$$X^b_{B_1A_2} = \frac{p}{T(p, R(d_{B_1A_2}))}\,. \tag{4.8}$$

If $X^b_{B_2A_2} < X^b_{A_1B_2}, X^b_{B_1A_2}$, then both flows are constrained by the shared link B_2A_2, and have equal throughput $X^b_{B_2A_2}$, given by (4.6).

In the general case, and assuming without loss of generality that $X^b_{A_1B_2} < X^b_{B_1A_2}$, the end-to-end throughput of the flow for each mesh network can be estimated from

$$X^b_A = \min(X^b_{A_1B_2}, X^b_{B_2A_2})\,, \tag{4.9}$$

$$X^b_B = \min(a \cdot X^b_A, X^b_{B_1A_2})\,, \tag{4.10}$$

where factor $a \geq 1$ is the ratio of the number of frames sent by network B over the number of frames sent by network A, in the same time interval. If the flow of network A is constrained by its first hop, i.e. $X^b_{A_1B_2} < X^b_{B_2A_2}$, then this flow will use less than its maximum throughput share on link B_2A_2. Whether the flow from network B can utilize the excess capacity depends on $X^b_{B_1A_2}$, as indicated in (4.10). The factor a in this case can be estimated from

$$X^b_A = \frac{p}{(a+1) \cdot T(p, R(d_{B_2A_2}))}\,, \tag{4.11}$$

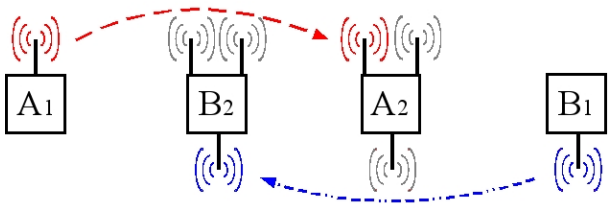

FIGURE 4.7: Multi-channel, 3-radio nodes, no mesh node sharing.

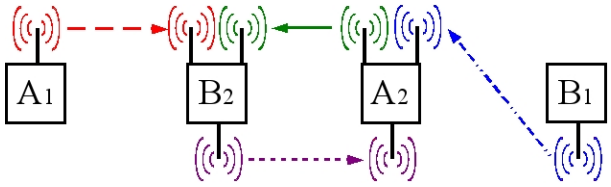

FIGURE 4.8: Multi-channel, 3-radio nodes, mesh node sharing.

where $X_A^b = X_{A_1B_2}^b$, which is given by (4.7). The denominator in the last equation depicts that within one sharing round of link B_2A_2, network A transmits one frame while network B transmits $a \geq 1$ frames.

Three-radio nodes: Now, a different channel can be assigned for each direction in the middle link, B_2A_2, Figure 4.8. The throughput of each direction can be approximated by

$$X_{B_2A_2}^b = \frac{p}{T(p, R(d_{B_2A_2}))} \ .$$

The throughput for links A_1B_2 and B_1A_2 is given by (4.7) and (4.8), respectively. Hence, the long-term end-to-end throughput of each mesh network can be estimated by

$$X_A^b = \min(X_{A_1B_2}^b, X_{B_2A_2}^b) \ ,$$

$$X_B^b = \min(X_{B_2A_2}^b, X_{B_1A_2}^b) \ .$$

For each of the multiple channel scenarios we can estimate the gain for both networks, using (4.1) and the pairs X_A^a, X_A^b and X_B^a, X_B^b for the case of no cooperation and cooperation, respectively. Note that the gain for the two networks may differ, hence there can be scenarios where cooperation is beneficial for only one of the networks.

4.3.2 Capacity Constraints

An important application of wireless mesh networks is to serve as access to wired networks, such as the Internet. It is not uncommon that the interconnection of a mesh network to the wired network is a bottleneck. This can be the case for DSL connections, whose speed depends on the distance of the subscriber to the provider's office where DSLAMs are located. Specifically, for

distances larger than 3 Km, the capacity for ADSL+ falls below 8 Mbps, which is significantly lower than the maximum throughput supported by 802.11a/g. In this section we extend the throughput model presented in Section 4.2, when there are constraints that are due to links external to the wireless mesh network.

4.3.2.1 Single Channel

Assume that the interconnection of mesh networks A and B to a wired network has maximum capacity C_A and C_B, respectively. Without loss of generality, we assume that $C_A < C_B$. The end-to-end throughput for mesh network A is

$$X^{C_A} = \min(C_A, X) \ , \tag{4.12}$$

where X is the throughput that is estimated by the model in Section 4.3, for either the case of no cooperation (*case a*) or cooperation (*case b*).

If $C_A < X$, then mesh network A uses less than its maximum share of the wireless channel, and mesh network B can potentially obtain a larger share. Hence, the end-to-end throughput of mesh network B is

$$X^{C_B} = \min(C_B, a \cdot X^{C_A}) \ ,$$

where factor $a \geq 1$ is the ratio of the number of frames sent by mesh network B over the number sent by network A, in the same time interval. In the case of no cooperation, factor a satisfies the equation

$$X^{C_A} = \frac{p}{T(p, R(d_{A_1A_2})) + a \cdot T(p, R(d_{B_1B_2}))} \ , \tag{4.13}$$

where X^{C_A} is given by (3.15). In the case of cooperation, factor a satisfies

$$X^{C_A} = \frac{p}{T(p, R(d_{A_1B_2})) + (a+1)T(p, R(d_{A_2B_2})) + a \cdot T(p, R(d_{B_1A_2}))} \ , \tag{4.14}$$

where as before, X^{C_A} is given by (3.15).

When both capacity constraints, C_A and C_B are lower than the throughput X^a given by (4.3), then the cooperation cannot be beneficial. Moreover, when both throughput constraints are greater than the throughput X^b given by (4.4), then the constraints do not affect cooperation, and the gains can be estimated by the model in Section 4.3.

4.3.2.2 Multiple Channels

Next we extend the multiple channel throughput model of Section 4.3.1, to account for capacity constraints external to the mesh network. We focus on the two-radio mesh node scenario; the extension to the other scenarios can be performed in a similar manner.

When there is no cooperation, the end-to-end throughput for mesh networks A and B is

$$X^{a,C_A} = \min(C_A, X_A^a) \ , \quad X^{a,C_B} = \min(C_B, X_B^a) \ ,$$

where X_A^a and X_B^a are given by (4.5). When the two networks cooperate, they share the middle link B_2A_2. The end-to-end throughput for networks A and B is now

$$\begin{aligned} X^{b,C_A} &= \min(C_A, X_A^b) \ , \\ X^{b,C_B} &= \min(C_B, X_{A_1B_2}^b, a \cdot X^{b,C_A}) \end{aligned} \tag{4.15}$$

where X_A^b is estimated by (4.9) and $X_{A_1B_2}^b$ is estimated by (4.7). Factor a satisfies the equation

$$X^{b,C_A} = \frac{p}{(a+1) \cdot T(p, R(d_{B_2A_2}))} \ ,$$

where X^{b,C_A} is estimated by (4.15).

4.4 Analytical Investigations

In this section, we present and discuss a series of analytical investigations using the models presented in the previous section. Our goal is to identify situations where there are performance incentives for cooperation between mesh operators, and quantify the corresponding throughput gains. This will provide insight on when and how much can be gained from cooperation.

The protocol overhead is important to precisely estimate the average throughput. A zero overhead, as assumed in (4.2), provides an upper bound of the throughput gains. For the analytical and simulation experiments we consider an overhead model based on the theoretical maximum throughput estimation in [JPS03]. This protocol overhead model is described in Appendix A.1.

The analytical models of Section 4.2 consider the transmission rate, which is a function of the distance between the transmitter and receiver, since it depends on the path loss between the two. For the following analytical experiments we use the physical layer model described in Appendix A.2. Unless otherwise noted, the experiments in this section consider the path loss exponent $n = 3$. The path loss model using this exponent give a maximum transmission range at the minimum rate equal to 368 meters for 802.11a, and equal to 541 meters for 802.11b.

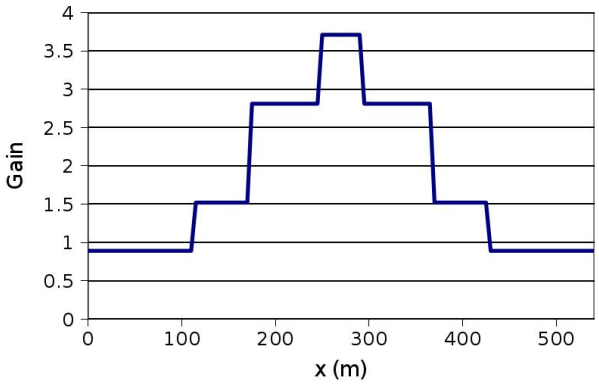

FIGURE 4.9: Throughput gain as a function of $x = d_{A_1B_2}$; $d_{A_1A_2} = d_{B_1B_2} = 541$ m, single channel, 802.11b.

4.4.1 Single Channel

In this section we investigate the gains in the single channel scenario of Section 4.3. We denote with d_{max} the maximum transmission range, which is 368 meters for 802.11a and 541 meters for 802.11b.

In the first experiment we set $d_{A_1A_2} = d_{B_1B_2} = d_{max}$. Figure 4.9 shows for 802.11b the end-to-end throughput gain for each mesh network that is achieved with cooperation, as a function of $x = d_{A_1B_2} \in [0, d_{max}]$. The throughput improves by more than three times in the best case scenario, which occurs when the distance $d_{A_1B_2}$ is approximately half of d_{max}. When the distance $d_{A_1B_2}$ is small, i.e. nodes A_1 and B_2 are close, then there are small or no advantages from cooperation, since the distance between A_1 and A_2 is close to that between B_2 and A_2, see Figure 4.2, hence the throughput achieved by these links is similar. Moreover, when the distance between A_1 and B_2 is close to d_{max}, then the throughput achieved by links A_1B_2 and A_1A_2 is similar, and again there are small or no gains from cooperation. The above explains the symmetry of the throughput gains in Figure 4.9 around the distance $x = d_{A_1B_2} \approx 270$ meters.

Figure 4.10 depicts the throughput gain achieved with cooperation in the case of 802.11a. Observe that the gain is lower than in 802.11b, however the improvements in terms of the absolute throughput is larger. This is partially due to the higher protocol overhead of 802.11a, and the larger number of intermediate transmission rates in 802.11a. Additionally, note that the range of values $x = d_{A_1B_2}$ with positive gains is larger than the corresponding range in the case of 802.11b, Figure 4.9. Observe in Figure 4.10 that as $x = d_{A_1B_2}$ increases from zero to $368/2 = 184$ meters, the throughput gain increases, except for a small drop at approximately 130 meters. This occurs for the following reason: as $d_{A_1B_2}$ increases the distance for links A_1B_2 and A_2B_1 increases, hence their rate decreases. At the same time, the distance of link A_2B_2 decreases, hence its rate increases. The drop in the gain occurs when the rate for links A_1B_2 and A_2B_1 decreases, before the rate for link A_2B_2 increases.

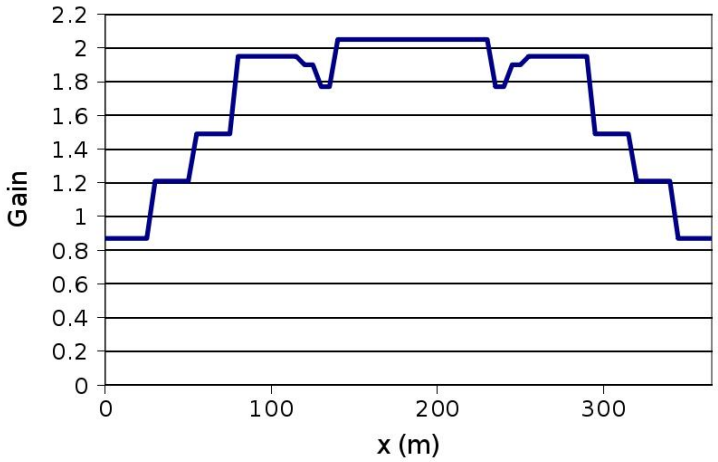

FIGURE 4.10: Throughput gain as a function of $x = d_{A_1B_2}$; $d_{A_1A_2} = d_{B_1B_2} = 368$ m, single channel, 802.11a.

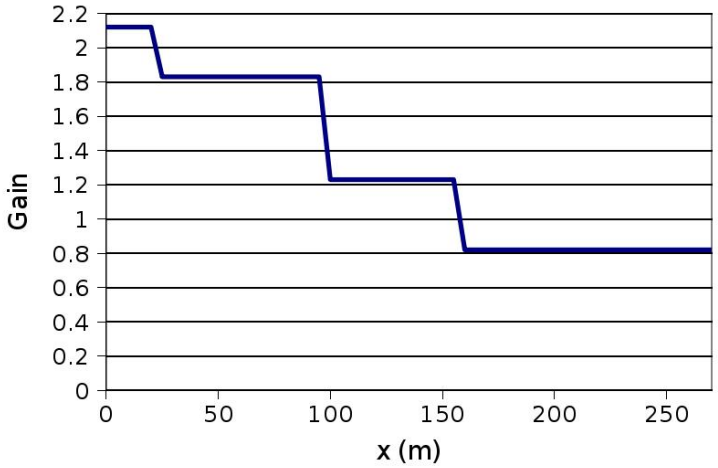

FIGURE 4.11: Throughput gain as a function of $x = d_{A_1B_2}$, when nodes A_1, A_2 can communicate at rate 11 Mbps; single channel, 802.11b

Next we consider $d_{A_1A_2} = d_{max}/2$, $d_{B_1B_2} = d_{max}$, and $x = d_{A_1B_2} \in [0, d_{max}/2]$. With these distances, the rate of link A_1A_2 is 11 Mbps, while the rate of B_1B_2 is 1 Mbps. Figure 4.11 shows the end-to-end throughput gain. Although the rate of link A_1A_2 is 11 Mbps and that of B_1B_2 is 1 Mbps, both mesh networks achieve equal gains, which are higher for smaller distances $d_{A_1B_2}$. This occurs because both networks share the same wireless channel.

In the next experiment we consider $x = d_{A_1A_2} = d_{B_1B_2}$ and $d_{A_1B_2} = x/2$, i.e. cooperation results in links with half the distance of those without cooperation. Figure 4.12 shows that cooperation is beneficial only for large distances $d_{A_1A_2}$, $d_{B_1B_2}$, for which the transmission rate is low.

Finally, Figure 4.13 shows that the throughput gain increases as the loss exponent n increases. Therefore, cooperation is expected to be more beneficial in environments with a high path loss.

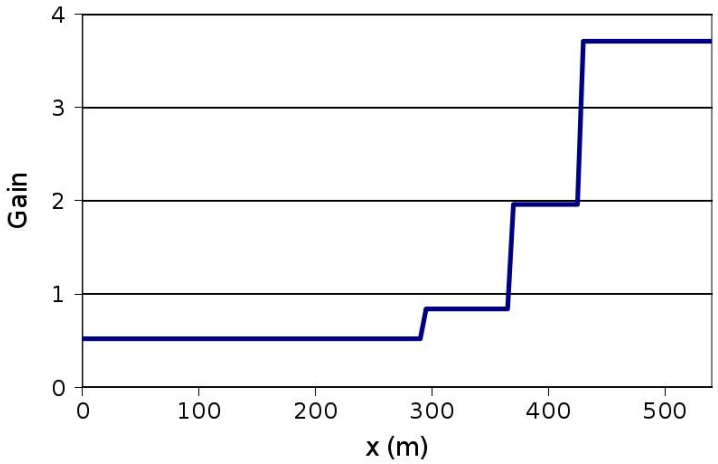

FIGURE 4.12: Throughput gain as a function of $x = d_{A_1A_2} = d_{B_1B_2}$, while $d_{A_1B_2} = x/2$; single channel, 802.11b

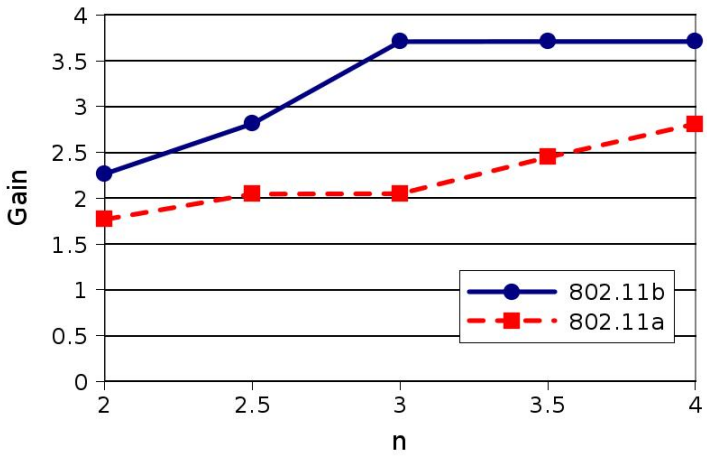

FIGURE 4.13: Throughput gain as a function of the path loss exponent; $d_{A_1A_2} = d_{B_1B_2} = d_{max}$, $d_{A_1B_2} = d_{max}/2$, single channel.

4.4.2 Multiple Channels

Next, we present experiments for the multiple channel scenario in Section 4.3.1. We focus on 802.11a, since it has more orthogonal channels available, which makes the multiple channel scenario more likely. As in the previous experiments, the frame payload is 1500 bytes. We repeat the first experiment of Section 4.4.1 for the case of 1, 2, and 3-radio mesh nodes. In particular, we set $d_{A_1A_2} = d_{B_1B_2} = d_{max} = 368$ meters, and investigate the throughput gain for various distances $x = d_{A_1B_2} \in [0, d_{max}]$. In all the experiments, the throughput gain for the two mesh networks is equal, since the topology is symmetric.

Figure 4.14 shows the throughput gain for single-radio mesh nodes. As discussed in Section 4.3.1, this case does not favor cooperation, since with cooperation all single-radio mesh nodes are required to operate on the same channel, whereas without cooperation the two mesh networks

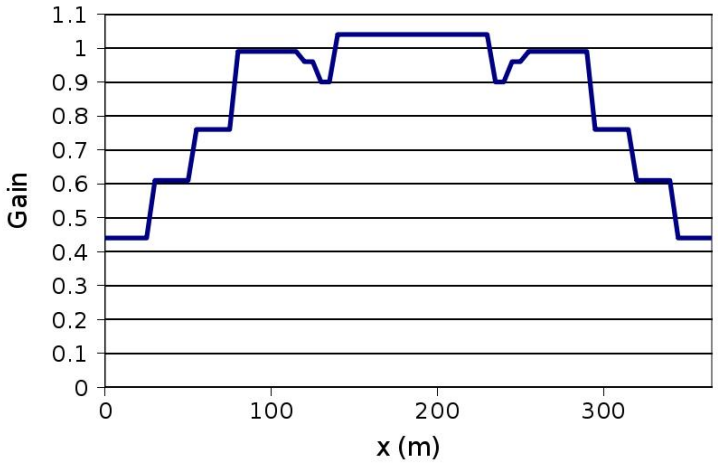

FIGURE 4.14: Throughput gain as a function of $x = d_{A_1B_2}$; $d_{A_1A_2} = d_{B_1B_2} = 368$ m, single-radio, 802.11a.

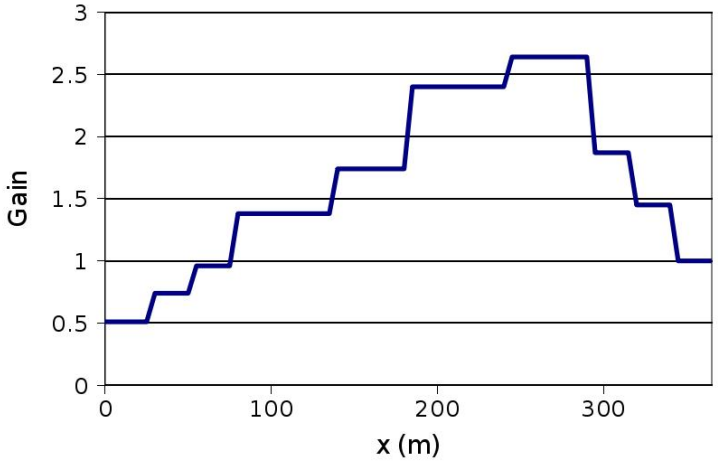

FIGURE 4.15: Throughput gain as a function of $x = d_{A_1B_2}$; $d_{A_1A_2} = d_{B_1B_2} = 368$ m, 2-radio, 802.11a.

can use orthogonal channels, hence reduce wireless channel contention. Despite the above, Figure 4.14 shows that there exist cases with a positive throughput gain, but this gain are very small (less than 5%).

Figure 4.15 depicts the results for the same experiment, in the case of 2-radio mesh nodes. Because the two mesh networks share link B_2A_2, the maximum throughput gain occurs when the capacity of this shared link is twice the capacity of links A_1B_2 and B_1A_2, which are used only by one network; the latter occurs when $x = d_{A_1B_2} \approx 250$ meters, in which case $d_{B_2A_2} \approx 368 - 250 = 118$ meters.

Figure 4.16 depicts the throughput gain in the case of 3-radio mesh nodes. Comparison of this figure with Figs. 4.15 and 4.14 indicate that the gains are higher for mesh nodes with more radios, which allows them to use more channels.

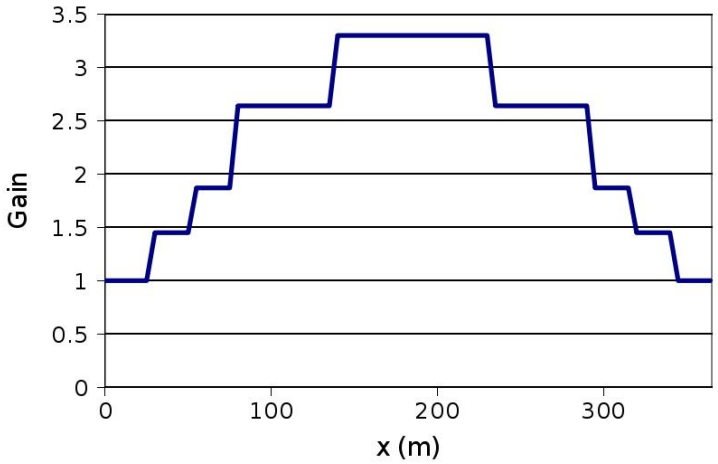

FIGURE 4.16: Throughput gain as a function of $x = d_{A_1B_2}$; $d_{A_1A_2} = d_{B_1B_2} = 368$ m, 3-radio, 802.11a.

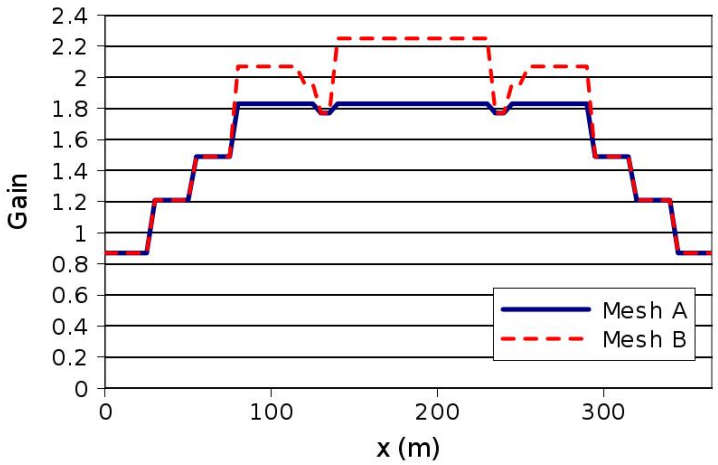

FIGURE 4.17: Throughput gain as a function of $x = d_{A_1B_2}$; $d_{A_1A_2} = d_{B_1B_2} = 541$ m, single channel, 802.11b, $C_A = 5$ Mbps.

4.4.3 Capacity Constraints

The following experiments refer to the single channel model with capacity constraints discussed in Section 4.3.2. We initially repeat the first experiment of Section 4.4.1, namely we set $d_{A_1A_2} = d_{B_1B_2} = d_{max} = 541$ meters, and investigate the throughput gain for various distances $x = d_{A_1B_2} \in [0, d_{max}]$. Additionally, we assume that mesh network A has a capacity constraint $C_A = 5$ Mbps. Figure 4.17 depicts the end-to-end throughput gain, which shows the values of x for which mesh network A is constrained, and network B uses the remaining channel. Comparison of Figure 4.17 with Figure 4.10 shows that, as expected, the maximum throughput gain for network A is smaller, due to its capacity constraint, whereas the gain for network B is higher, since it can increase its throughput share, exploiting A's underutilization of its maximum share, due to its capacity constraint.

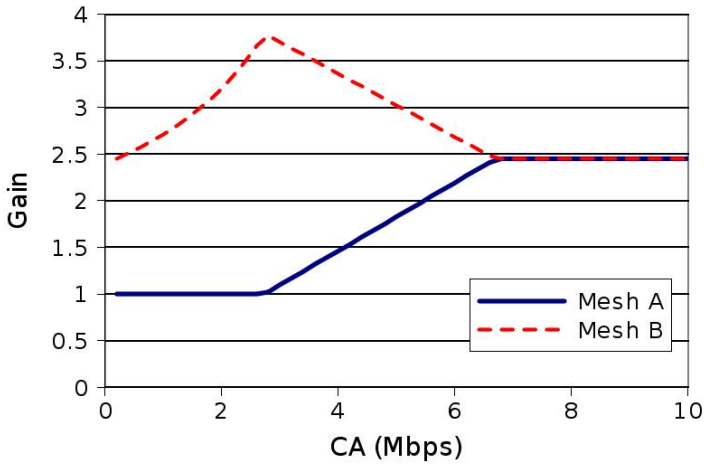

FIGURE 4.18: Throughput gain as a function of C_A; $d_{A_1B_2} = 270$ m, $d_{A_1A_2} = d_{B_1B_2} = 541$ m, single channel, 802.11b.

TABLE 4.1: Transmission rates (in Mbps) for various links, in different experiments.

Exp. ID	$R(d_{A_1B_2})$	$R(d_{B_2A_2})$	$R(d_{A_2B_1})$
1	11	1	11
2	11	2	11
3	11	5.5	11
4	11	11	11
5	5.5	11	5.5
6	2	11	2
7	1	11	1

In the next experiment we set $d_{A_1B_2} = d_{max}/2$, which yields the highest gain in Figure 4.17. Figure 4.18 shows the throughput gain for different values of C_A. This figure contains three regions with a different behavior of the gain for networks A and B: For $C_A < 2.5$ Mbps, there are no gains for network A. Interestingly, observe that as C_A increases, the gain for network B increases, indicating that when there is a higher contention, which occurs when C_A increases since network A can transmit more traffic, cooperation yields larger improvements. For 2.5 Mbps $< C_A <$ 6.5 Mbps, there is a positive gain for network A, which increases as the capacity constraint increases; at the same time, the gain for network B decreases. Finally, for $C_A > 6.5$ Mbps, C_A is larger than the maximum capacity supported by the wireless mesh network, hence does not affect the gain, which is the same for both mesh networks.

4.5 Simulation Evaluation

In this section we present simulation experiments based on NS-2, to validate the throughput model presented in Section 4.2 and verify that it can accurately estimate the throughput gains

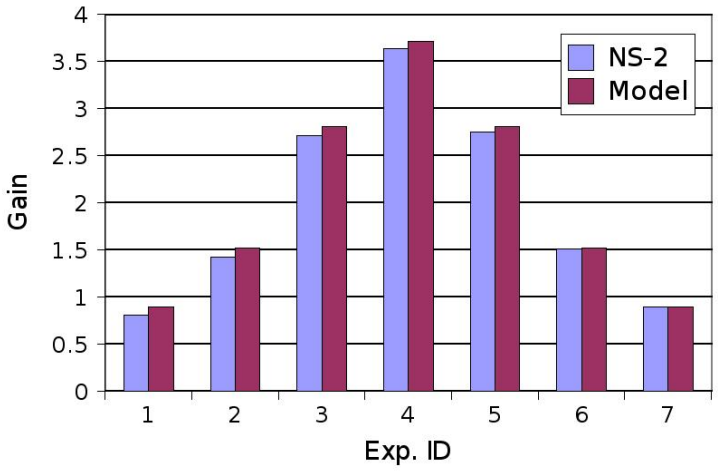

FIGURE 4.19: Gain based on analysis and simulation.

that are achieved through cooperation. The default version of NS-2 does not support multiple rates for transmissions between one transmitter and multiple receivers. Hence, we extended NS-2 to support multiple rates by adapting the transmission rate according to the signal strength of the last received frame.

We consider the single channel scenario in 802.11b, whose throughput model is presented in Section 4.3. Note that this scenario has the most transmitters contending for channel access; this observation together with the fact that the proposed throughput models do not account for collisions, makes this the most likely scenario, among all the scenarios considered in this section, to exhibit inaccuracies of the analytical model. The distances $d_{A_1A_2}$ and $d_{B_1B_2}$ where selected so that the corresponding links achieved transmission rate 1 Mbps. Moreover, the distances $d_{A_1B_2}$, $d_{B_2A_2}$, and $d_{A_2B_2}$ were set in order to achieve the transmission rates shown in Table 4.1, which correspond to different throughput gains in Figure 4.9. The simulation results shown below are the average of 100 runs with the same parameters. The experiments used UDP traffic, and each run had duration 15 seconds.

Figure 4.19 shows that the analytical results for the throughput gain closely match the corresponding simulation results, verifying that the analytical throughput model can accurately estimate the throughput gains.

4.6 Conclusions

In this chapter we have investigated the incentives for cooperation between wireless mesh network operators, due solely to the performance improvements that cooperation yields for both operators. The analytical framework presented can identify when such improvements exist, and

quantify them. The analytical models include cases of single channel operation, multiple channel operation with multi-radio mesh nodes, and the case of capacity constraints external to the wireless mesh network. The accuracy of the analytical models has been verified with simulation.

Chapter 5

Conclusions and Further Work

5.1 Conclusions

Even in competitive environments where each party acts at its own self-interest, it is shown that there are scenarios that the cooperation between competitive operators can yield benefits to both of them. As a result, this performance gain raises incentives that can motivate cooperation without any agreement that includes monetary exchange. In WLANs, serving the clients of the neighboring access point that belongs to a different operator, can significantly increase the performance of both networks including the new host network. Moreover, sharing mesh nodes between WMNs that belong to different operators, can significantly improve the end-to-end throughput of both networks.

The proposed analytical framework is able to approximate the end-to-end throughput in each case and predict whether the cooperation is expected to be beneficial and estimate the expected gain. In either the case of handovers in WLANs or mesh node sharing in WMNs, the analytical framework includes models for various topologies, scenarios with capacity constraints outside the wireless medium, scenarios where there are no saturated conditions and multi-channel and multi-radio scenarios. The accuracy of the model is verified through simulations and real experiments. The simulations suggest that modeling framework may misestimate whether the cooperation is beneficial. However, misestimations appear in scenarios where the gain / loss is marginal. Hence, the small number of false positives and false negatives do not affect the long-term benefits of the cooperation and the reliability of the model.

5.2 Further Work

Future work includes a generic throughput approximation model that can accurately estimate the end-to-end throughput in any possible topology. A key challenge of this problem is the existence of hidden and exposed nodes [JPDG04].

It is also interesting to investigate the effects of the recently standardized IEEE 802.11n protocol to resource sharing incentives. A key feature of 802.11n is is to increase throughput by using wider bands and multiple antennas (MIMO) [Xia05]. As a result, in 802.11n environments, there is an increased probability that two overlapping networks interfere with each other, which can increasingly lead to cases that give rise to the tradeoffs identified in the sharing models investigated in this thesis.

Finally, further work includes a proof-of-concept implementation of the proposed procedure based on the principles discussed in Section 3.7.

Appendix A

Auxilliary Models

A.1 Protocol Overhead Model

For the analytical and simulation experiments we consider an overhead model based on the theoretical maximum throughput estimation in [JPS03]. In this Appendix we discuss this overhead model, and extend the backoff overhead to account for multiple contending transmissions. Note that the overhead model does not capture collisions; its accuracy for estimating the throughput gains is evaluated using simulations and real experiments in Sections 3.6 and 4.5.

We consider the standard DCF (Distributed Coordination Function) protocol without RTS/CTS. The time for transmitting one frame consists of five components: T_{DIFS}, T_{SIFS}, T_{ACK}, T_{BO}, and T_{DATA}. The IFS delays are defined by the standard. T_{ACK} is the time for transmitting an acknowledgment, which in 802.11a is transmitted with the same transmission rate as a data frame, while in 802.11b it is transmitted at the minimum rate. T_{BO} is the duration of the backoff, which we further discuss below. Finally, T_{DATA} is the time for transmitting one frame, which includes the MAC and physical layer headers, and the frame payload.

Based on the above, we can define $T(p, R)$ that appears in the models of the previous section as follows:

$$T(p, R) = T_{DIFS} + T_{SIFS} + T_{ACK}^{R} + T_{DATA}^{p,R} \,. \tag{A.1}$$

Note that the backoff time T_{BO} is not included in the above expression, since it is not an overhead that needs to be added to each frame transmission. Rather, it needs to be added to the denominator of the throughput expressions presented in the previous section. When there is a single transmitter, the expected backoff delay is equal to $CW_{min}/2$ time slots, where the minimum contention window CW_{min} and the time slot duration are defined by the standard. When there are multiple contending transmitters, their backoff counter decreases simultaneously, since the backoff counter freezes when a transmission is sensed. Based on this and as long as no

TABLE A.1: Delay components for transmitting one frame in 802.11a.

802.11a	time (μs)
T_{DIFS}	34
T_{SIFS}	9
T^1_{BO}	67.5
T_{ACK}	$20 + 4 \cdot \lceil 16 + 6 + 8 \cdot 14/(4 \cdot R) \rceil$
T_{DATA}	$20 + 4 \cdot \lceil 16 + 6 + 8 \cdot (34 + p)/(4 \cdot R) \rceil$

TABLE A.2: Delay components for transmitting one frame in 802.11b.

802.11b	time (μs)
T_{DIFS}	50
T_{SIFS}	10
T^1_{BO}	310
T_{ACK}	304
T_{DATA}	$192 + 8 \cdot (34 + p)/R$

collisions occur, the total backoff delay is independent of the number of contending transmitters, and depends only on the maximum number of frames a single transmitter sends in the time interval over which the throughput is estimated. Hence, the backoff delay is qT^1_{BO}, where $T^1_{BO} = CW_{min}/2$ is the average backoff delay when there is only one transmitter, and q is the maximum number of frames sent by a single transmitter. The value of q is 1 in all the equations, except for (3.16), (3.17), (3.19) and (3.20) in Chapter 2 and (4.11), (4.13) and (4.14) in Chapter 3 where $q = a$.

Table A.1 and A.2 shows the values of T_{DIFS}, T_{SIFS}, T^1_{BO}, T_{ACK} and T_{DATA} for 802.11a and 802.11b respectively, according to [JPS03]. The frame payload size p is in bytes and the rate R is in Mbps. In all the experiments we consider payload size $p = 1500$ bytes.

A.2 Physical Layer Model

The analytical models of Section 4.2 consider the transmission rate, which is a function of the distance between the transmitter and receiver, since it depends on the path loss between the two. We consider the link budget equation for estimating the signal power at the receiver:

$$P_{rx} = P_{tx} + G_{tx} - LL_{tx} + G_{rx} - LL_{rx} - PL \ , \tag{A.2}$$

where P_{rx} is the signal power at the receiver in dBm, P_{tx} is the output power of the transmitter in dBm, G_{tx} and G_{rx} are the transmitter and the receiver antenna gains, respectively, in dBi,

TABLE A.3: Sensitivity thresholds for 802.11a

Rate (Mbps)	6	9	12	18	24	36	48	54
Threshold (dBm)	-88	-87	-86	-85	-82	-79	-74	-73

TABLE A.4: Sensitivity thresholds for 802.11b

Rate (Mbps)	1	2	5.5	11
Threshold (dBm)	-96	-93	-91	-88

LL_{tx} and LL_{rx} are the antenna and cable losses at the transmitter and receiver in dB, and PL is the propagation path loss in dB.

In the experiments, we consider 6 dBi omni-directional antennas and transmission power 24 dBm and 14 dBm for 802.11a and 802.11b, respectively. These values are in agreement with the ETSI's EIRP (Equivalent Isotropic Radiated Power) indoor and outdoor limits for the EU[1]. We also assume that the antenna and cable losses are negligible (or are included in the antenna gains). The path loss is calculated using the following equation:

$$PL = P_1 + 10 \log_{10} d^n \ ,$$

where d is the distance between the receiver and the transmitter in meters, n is the loss exponent and P_1 is the path loss for the first meter. P_1 is estimated according to the free space path loss formula

$$FSPL(dB) = 32.44 + 20 \log_{10}(f) + 20 \log_{10}(d) \ ,$$

where f is the frequency in GHz and d is the distance in meters. Hence, we take P_1 to be 47 dB in 802.11a and 40 dB in 802.11b. In 802.11a the path loss is 7 dB greater than 802.11b, because the frequency of the former is almost double.

A successful packet transmission requires that the received signal power estimated by (A.2) is higher than the receiver sensitivity threshold. We use the sensitivity thresholds of Cisco's Aironet 1240AG [Sys] access point, which are shown in Tables A.3 and A.4.

The path loss model (A.2) using a loss exponent $n = 3$, and the sensitivity thresholds in Tables A.3 and A.4, give a maximum transmission range at the minimum rate equal to 368 meters for 802.11a, and equal to 541 meters for 802.11b.

[1]Radio and Telecommunications Terminal Equipment (R&TTE) Directive 1999/5/EC, `www.rtte.net`

Bibliography

[AE03] Luzi Anderegg and Stephan Eidenbenz. Ad Hoc-VCG: A Truthful and Cost-Efficient Routing Protocol for Mobile Ad Hoc Networks with Selfish Agents. In *MOBICOM '03: Proceedings of the 9th ACM Annual International Conference on Mobile Computing and Networking*, pages 245–259, 2003.

[AJSS05] Aditya Akella, Glenn Judd, Srinivasan Seshan, and Peter Steenkiste. Self-Management in Chaotic Wireless Deployments. In *MOBICOM '05: Proceedings of the 11th ACM Annual International Conference on Mobile Computing and Networking*, pages 185–199, 2005.

[BCL+08] Paramvir Bahl, Ranveer Chandra, Patrick P. C. Lee, Vishal Misra, Jitendra Padhye, Dan Rubenstein, and Yan Yu. Opportunistic Use of Client Repeaters to Improve Performance of WLANs. In *CoNEXT '08: Proceedings of the 4th ACM International Conference on emerging Networking EXperiments and Technologies*, pages 1–12, 2008.

[BH03] Levente Buttyán and Jean-Pierre Hubaux. Stimulating Cooperation in Self-organizing Mobile Ad Hoc Networks. *ACM/Kluwer Mobile Networks and Applications*, 8(5):579–592, 2003.

[BPK+07] Ioannis Broustis, Konstantina Papagiannaki, Srikanth V. Krishnamurthy, Michalis Faloutsos, and Vivek Mhatre. MDG: Measurement-Driven Guidelines for 802.11 WLAN Design. In *MOBICOM '07: Proceedings of the 13th annual ACM international conference on Mobile computing and networking*, pages 254–265, 2007.

[ByLB02] Sonja Buchegger and Jean yves Le Boudec. Performance Analysis of the CONFIDANT Protocol: Cooperation Of Nodes - Fairness In Dynamic Ad-Hoc NeTworks. In *MOBIHOC '02: Proceedings of the 3rd ACM International Symposium on Mobile Ad Hoc Networking and Computing*, pages 226–236, 2002.

[CGKO04] Jon Crowcroft, Richard Gibbens, Frank Kelly, and Sven Östring. Modelling Incentives for Collaboration in Mobile Ad Hoc Networks. *Performance Evaluation*, 57(4):427–439, 2004.

[DPZ04] Richard Draves, Jitendra Padhye, and Brian Zill. Routing in Multi-Radio, Multi-Hop Wireless Mesh Networks. In *MOBICOM '04: Proceedings of the 10th ACM Annual International Conference on Mobile Computing and Networking*, pages 114–128, 2004.

[DVR03] Suman Das, Harish Viswanathan, and Gee Rittenhouse. Dynamic Load Balancing Through Coordinated Scheduling in Packet Data Systems. In *INFOCOM '03: Proceedings of the 22th IEEE International Conference on Computer Communications*, pages 786–796, 2003.

[FCH+07] Laura Marie Feeney, Bilge Cetin, Daniel Hollos, Martin Kubisch, Seble Mengesha, and Holger Karl. Multi-Rate Relaying for Performance Improvement in IEEE 802.11 WLANs. In *WWIC '07: Proceedings of the 5th International Conference on Wired/Wireless Internet Communications*, 2007.

[FRBsD03] Martin Heusse Franck, Franck Rousseau, Gilles Berger-sabbatel, and Andrzej Duda. Performance Anomaly of 802.11b. In *INFOCOM '03: Proceedings of 22th IEEE International Conference on Computer Communications*, pages 836–843, 2003.

[FS09a] Xenofon Fafoutis and Vasilios A. Siris. Cooperation Incentives between Wireless Mesh Network Operators. In *Proceedings of the 3rd ERCIM Workshop on eMobility*, pages 99–100, 2009.

[FS09b] Xenofon Fafoutis and Vasilios A. Siris. Handover Incentives for WLANs with Overlapping Coverage. In *WWIC '09: Proceedings of the 7th International Conference on Wired/Wireless Internet Communications*, pages 146–158, 2009.

[FS10] Xenofon Fafoutis and Vasilios A. Siris. Performance Incentives for Cooperation between Wireless Mesh Network Operators. In *CARMEN '10: To Appear in 2nd International Workshop on Carrier Grade Wireless Mesh Networks*, 2010.

[GS08] Manolis Genetzakis and Vasilios A. Siris. A Contention-Aware Routing Metric for Multi-Rate Multi-Radio Mesh Networks. In *SECON '08: Proceedings of the 5th Annual IEEE Communications Society Conference on Sensor, Mesh and Ad Hoc Communications and Networks*, pages 242–250, 2008.

[JPDG04] Aruna Jayasuriya, Sylvie Perreau, Arek Dadej, and Steven Gordon. Hidden vs. Exposed Terminal Problem in Ad hoc Networks. In *ATNAC '04: Proceedings of Australian Telecommunication Networks and Applications Conference*, 2004.

[JPS03] Jangeun Jun, Pushkin Peddabachagari, and Mihail L. Sichitiu. Theoretical Maximum Throughput of IEEE 802.11 and its Applications. In *NCA '03: Proceedings of 2nd IEEE International Symposium on Network Computing and Application*, pages 249–257, 2003.

[KAMG07] Anurag Kumar, Eitan Altman, Daniele Miorandi, and Munish Goyal. New Insights from a Fixed-Point Analysis of Single Cell IEEE 802.11 WLANs. *IEEE/ACM Transactions on Networking*, 15(3):588–601, 2007.

[KBC+07] Bruno Kauffmann, François Baccelli, Augustin Chaintreau, Vivek Mhatre, Konstantina Papagiannaki, and Christophe Diot. Measurement-Based Self Organization of Interfering 802.11 Wireless Access Networks. In *INFOCOM '07: Proceedings of 26th IEEE International Conference on Computer Communications*, pages 1451–1459, 2007.

[KK05] Anurag Kumar and Vinod Kumar. Optimal Association of Stations and APs in an IEEE 802.11 WLAN. In *NCC '05: Proceedings of the 11th annual National Conference on Communications*, 2005.

[KKN06] Gaurav S. Kasbekar, Joy Kuri, and Pavan Nuggehalli. Online Association Policies in IEEE 802.11 WLANs. In *WiOpt '06: Proceedings of 4th International Symposium on Modeling and Optimization in Mobile, Ad Hoc and Wireless Networks*, pages 1–10, 2006.

[KLBK08] Srikanth Kandula, Kate Ching-Ju Lin, Tural Badirkhanli, and Dina Katabi. FatVAP: Aggregating AP Backhaul Capacity to Maximize Throughput. In *NSDI '08: Proceedings of the 5th USENIX Symposium on Networked Systems Design and Implementation*, pages 89–104, 2008.

[KS08] Ioannis Koukoutsidis and Vasilios A. Siris. Access Point Assignment Algorithms in WLANs based on Throughput Objectives. In *WiOpt '08: Proceedings of 6th International Symposium on Modeling and Optimization in Mobile, Ad Hoc and Wireless Networks*, pages 375–383, 2008.

[KV06] Pradeep Kyasanur and Nitin H. Vaidya. Routing and Link-Layer Protocols for Multi-Channel Multi-Interface Ad Hoc Wireless Networks. *ACM SIGMOBILE Mobile Computing and Communications Review*, 10(1):31–43, 2006.

[LL05] Jain-Shing Lue and Chun-Hung Richard Lin. An Opportunistic Relay Method for Increasing Throughput in Multirate IEEE 802.11 wireless LAN. *IEICE Transactions on Communications*, E88-B(6):2672–2675, 2005.

[LTN+07] Pei Liu, Zhifeng Tao, Sathya Narayanan, Thanasis Korakis, and Shivendra S. Panwar. CoopMAC: A Cooperative MAC for Wireless LANs. *IEEE Journal on Selected Areas in Communications*, 25(2), 2007.

[MCH+03] Stefan Mangold, Sunghyun Choi, Guido R. Hiertz, Ole Klein, and Bernhard Walke. Analysis of IEEE 802.11e for QoS Support in Wireless LANs. *IEEE Wireless Communications*, 10(6):40–50, 2003.

[NLP05] Sathya Narayanan, Pei Liu, and Shivendra S. Panwar. On the Advantages of Multi-Hop extentions to the IEEE 802.11 Infrastracture Mode. In *WCNC '05: Proceedings of IEEE Wireless Communications and Networking Conference*, 2005.

[SS06] Vasilios A. Siris and George Stamatakis. Optimal CWmin Selection for Achieving Proportional Fairness in Multi-Rate 802.11e WLANs: Test-Bed Implementation and Evaluation. In *WiNTECH '06: Proceedings of the 1st International Workshop on Wireless Network Testbeds, Experimental Evaluation & Characterization*, pages 41–48, 2006.

[Sys] Cisco Systems. Aironet 1240AG Series 802.11A/B/G Access Point. In `http://www.cisco.com/en/US/products/ps6521/`.

[TG04] Godfrey Tan and John Guttag. Time-Based Fairness Improves Performance in Multi-Rate WLANs. In *ATEC '04: Proceedings of the Annual Conference on USENIX Annual Technical Conference*, pages 23–23, 2004.

[Xia05] Yang Xiao. IEEE 802.11n: Enhancements for Higher Throughput in Wireless LANs. *IEEE Wireless Communications*, 12(6):82–91, 2005.

[ZCY03] Sheng Zhong, Jiang Chen, and Richard Yang. Sprite: A Simple, Cheat-Proof, Credit-Based System for Mobile Ad-Hoc Networks. In *INFOCOM '03: Proceedings of 22th IEEE International Conference on Computer Communications*, pages 1987–1997, 2003.